High density linkage to physical mapping in a unique Tall x Dwarf Coconut (*Cocos nucifera* L.) outbred F_2 uncovers a major QTL for flowering time colocalized with the *FLOWERING LOCUS T (FT)*

Dario Grattapaglia[1,2], Wellington Bruno dos Santos Alves[1,2] and Cleso Antônio Patto Pacheco[3]

[1]EMBRAPA Recursos Genéticos e Biotecnologia, Brasília, DF, Brazil
[2]Programa de Ciências Genômicas e Biotecnologia, Universidade Católica de Brasília, Brasília, DF, Brazil
[3]EMBRAPA Tabuleiros Costeiros, Aracaju, SE

ORCID
Dario Grattapaglia: 0000-0002-0050-970X
Wellington Bruno dos Santos Alves: 0000-0002-4915-0283

*Corresponding author: dario.grattapaglia@embrapa.br

Word count: 7573 words
Number of tables: 2
Number of figures: 6
Supplementary files: 8

Abstract

Introduction: The coconut tree crop (*Cocos nucifera* L.) provides vital resources for millions of people worldwide. Coconut germplasm is largely classified into 'Tall' (Typica) and 'Dwarf' (Nana) types. While Tall coconuts are outcrossing, more productive, stress tolerant and late flowering, Dwarf coconut are inbred, flower early with a high rate of bunch emission. Precocity determines earlier production of a plantation and facilitates management and harvest.

Methods: We used a unique outbred F_2 population generated by intercrossing F_1 hybrids between Brazilian Green Dwarf from Jiqui (BGDJ) and West African Tall (WAT) cultivars. SNP markers fixed for alternative alleles in the two varieties, segregating in an F_2 configuration were used to build a high-density linkage map with ~3,000 SNPs, anchored to the existing chromosome-level genome assemblies, and a QTL mapping analysis was carried out.

Results: The linkage map established the chromosomes numbering correspondence between the two reference genome versions and the relationship between recombination rate, physical distance and gene density in the coconut genomes. Leveraging the strong segregation for precocity inherited from the Dwarf cultivar in the F_2, a major effect QTL with incomplete dominance was mapped for flowering time. *FLOWERING LOCUS T* (*FT*) gene homologs of coconut previously described as putatively involved in flowering time by alternative splice variant analysis, were colocalized within a ~200kb window of the major effect QTL (LOD=11.86).

Discussion: Our work provides strong phenotype-based evidence for the role of the FT locus as the putative underlying functional variant for the flowering time difference between Dwarf and Tall coconuts. Major effect QTLs were also detected for developmental traits of the palm, plausibly suggesting pleiotropism of the *FT* locus for other precocity traits. Haplotypes of the two SNPs flanking the flowering time QTL inherited from the Dwarf parent BGDJ caused a reduction in the time to flower of around 400 days. These SNPs could be used for high throughput marker assisted selection of early flowering and higher productivity recombinant lines, providing innovative genetic material to the coconut industry.

Keywords: Coconut, *FLOWERING LOCUS T*, hybrid breeding, SNPs, flowering

Running title: A flowering time QTL colocalized with FLOWERING LOCUS T in coconut

1. Introduction

The coconut palm (*Cocos nucifera* L.) is a worldwide important tropical tree crop providing vital resources for millions of farmers and industries with a diverse use of its oil and fruit products. The only species belonging to the genus *Cocos*, the coconut palm is a diploid (2n = 32) monoecious, perennial monocotyledon of the family *Arecaceae* (Palmae), with a relatively large genome size (1C = 2.74 Gb). With its most likely center of origin in Southeastern Asia, it is currently cultivated in more than 92 tropical countries (Batugal et al., 2009; Gunn et al., 2011) covering more than 12 million hectares worldwide (FAO, 2021).

69 Coconut germplasm is largely classified into 'Tall' (Typica) and 'Dwarf' (Nana)
70 types. Tall, a.k.a. Giant coconuts, are preferentially outcrossing, genetically diverse and
71 display high productivity, broad adaptability and tolerance to specific pests and
72 diseases. Dwarf coconuts are mostly self-pollinating with limited genetic diversity
73 within each variety but are chosen for their precocity and high rate of bunch emission.
74 Early flowering of the dwarf varieties is a feature of great agronomic relevance that
75 results not only in precocity of nut harvest, but also increased production, while
76 facilitating coconut tree management and harvest operations. While the tall (late)
77 variety takes an average of 8 years to flower, the early flowering dwarfs typically
78 flower on average 2 to 4 years after planting (Perera et al., 2016). The origin of dwarf
79 coconuts has been a matter of debate, although current consensus based on molecular
80 studies points toward a process of domestication from the ancestral tall coconut
81 possibly following the appearance of mutations in flowering time genes resulting in
82 autogamy (Perera et al., 2016), as well gibberellin biosynthesis affecting height growth
83 (Boonkaew et al., 2018; Wang et al., 2021).

84 Notwithstanding its global socioeconomic importance, advances in coconut
85 tree improvement have been modest, hindered by its perennialism, long generational
86 time, late flowering and large tree size, which demand extensive experimental areas
87 and continuous long-term investments. Genetic improvement programs have adopted
88 two main breeding strategies: (1) intravarietal breeding coupled to mass selection and
89 (2) intervarietal hybridization, the most widely used strategy, which consolidates, into
90 an intermediate F_1 hybrid, the key features of each variety, such as precocity and short
91 stature from the dwarfs and the rusticity and production of larger fruits from the tall
92 varieties (Batugal et al., 2009; Perera et al., 2016). Rare have been studies in F_2

93 populations derived either from selfing or cross pollination among F_1 Tall x Dwarf
94 hybrids. The wide segregation for production traits reported in F_2 generations has
95 discouraged such endeavors. Time to flowering, pollination behavior, height and the
96 presence of bole - an expansion at the base of the stem - have been considered to
97 segregate independently. While the former two traits showed the involvement of
98 several genes, height and bole character segregation suggested the presence of at
99 least one major gene each, with incomplete dominance (Fernando and Perera, 1997;
100 Namboothiri et al., 2011; Perera et al., 2016), although no genetic follow-up testing of
101 such hypothesis was ever reported.

102 Advances in mapping quantitative trait loci (QTLs) of economically important
103 traits have been limited in coconut, restricted to a few studies using Tall x Dwarf F_1
104 hybrid populations (Herrán et al., 2000; Ritter et al., 2000; Lebrun et al., 2001;
105 Baudouin et al., 2006; Riedel et al., 2009). In such F_1 experimental populations,
106 segregating variation can only be captured from the outbred tall coconut, because the
107 dwarf parent, being essentially an inbred line, will not contribute allelic segregation.
108 Flowering time as well as other traits related to the dwarf behavior typically display an
109 intermediate phenotype in the F_1 progeny with no segregation that would allow
110 genetic mapping of major effects contributed by the dwarf genotype. Studies of F_2 or
111 backcross populations are needed to advance the molecular understating of key traits
112 related to precocity in coconut. Furthermore, genetic mapping in the cited studies has
113 been carried out either with low portability AFLP markers or a limited set of
114 microsatellites, which do not provide adequate sequence-level information for deeper
115 investigation of putative genes underlying mapped QTLs. Only recently has this
116 scenario begun to change with studies employing single nucleotide polymorphism

117 (SNP) markers for diversity studies (Muñoz-Pérez et al., 2022), linkage mapping to
118 support genome assembly (Yang et al., 2021), and whole genome sequencing for
119 genome-wide studies (GWAS) (Wang et al., 2021). Understanding the genetic basis of
120 morphological traits that determine precocity with a particular interest in early
121 flowering, would represent an important step towards breeding advancement of
122 coconut.

123 In the present study, we used a unique mapping approach in an outbred F_2
124 population generated by open pollination intercrossing F_1 hybrid trees between the
125 Brazilian Green Dwarf from Jiqui (BGDJ) and the West African Tall (WAT). We exploited
126 the fact that the Dwarf variety is essentially a fixed inbred line with very little if any
127 heterozygosity, while the Tall variety is genetically diverse. Following interbreeding of
128 the F_1 trees, SNP markers fixed in homozygosity in the Tall variety for the alternative
129 allele to the one fixed in the Dwarf will segregate in a 1:2:1 ratio providing a very large
130 number of loci segregating in a bona fide F_2 configuration to allow mapping the
131 quantitative variation underlying the genetic divergence between tall and dwarf
132 coconut types. This SNP selection strategy essentially converted the outbred F_2
133 population into a standard F_2, allowing the appropriate application of linkage and QTL
134 mapping. We built a high-density linkage map using SNPs derived from genotyping by
135 sequencing with DArTseq, aligned the map to the current genome assemblies and
136 located QTLs for traits related to precocity, including a major effect locus for flowering
137 time colocalized with the *FLOWERING LOCUS T* (*FT*).

138 # 2. Materials and methods

139 ## 2.1 Plant material and DNA extraction

140 The study was carried out with 182 F_2 plants, generated by open pollination
141 interbreeding among PB-141 F_1 coconut hybrid plants in a ten-year-old commercial
142 plantation managed by Embrapa Tabuleiros Costeiros, Aracaju – SE (10.9513° South,
143 37.0528° West). PB-141 is an F_1 hybrid derived from the cross between the Brazilian
144 Green Dwarf from Jequi (BGDJ) and West African Tall (WAT). Coconuts were collected
145 from F_1 palms in the central area of the commercial plantation in order to maximize
146 the probability of being effectively derived from intercrossing of F_1 plants. F_2 plants
147 were therefore derived either from selfing or cross pollination between different F_1
148 plants. Samples of young leaves were collected and used to extract total genomic DNA
149 using an optimized Sorbitol-CTAB-based protocol (Inglis et al., 2018). DNA
150 concentrations and purity were estimated using a Nanodrop 2000
151 spectrophotometer (Thermo Scientific).

152 ## 2.2 SNP genotyping

153 Genomic DNA samples were shipped to the Service of Genetic Analysis for
154 Agriculture (SAGA) laboratory in Mexico for high-throughput genotyping using the
155 DArTSeq method developed by Diversity Arrays Technology Pty Ltd. (Sansaloni et al.,
156 2011). DNA complexity reduction was performed using the SbfI/MseI enzyme
157 combination. Samples were processed in digestion/ligation reactions and the
158 scrambled fragments were amplified using two primers with sequence complementary
159 to the ligated adapters and oligonucleotides from the sequencing platform.
160 Subsequently, the clusters were sequenced on an Illumina HiSeq2500 sequencing

161 platform. SNP markers were detected following mapping of sequence reads sampled
162 at adequate depth on the Coconut reference genome (Yang et al., 2021) according to
163 standard parameters defined in DArTsoft14, an automated genomics data analysis
164 program and DArTdb, a laboratory management system developed and patented by
165 DArT for generating SNP marker data. Following the standard scoring system provided
166 by the DArTsoft14 platform, codominant SNP markers were scored as "0" for
167 homozygous reference allele, "1" for homozygous alternative allele, and "2" for
168 presence of both the reference and the alternative allele. These scores were later
169 converted to the corresponding genotypic classes with formats hh, kk and hk
170 respectively, for linkage mapping under an unknown linkage phase configuration (see
171 below).

172 2.3 Morphological and flowering trait evaluations

173 Due to restrictions in field availability for planting, only 125 of the 182 F_2 plants
174 were ultimately planted in a field trial in a site known for its soil homogeneity at
175 Embrapa Tabuleiros Costeiros research center in June, 2018. Since no replicate plants
176 were possible for the 125 F_2 plants (n =125 entries), these were deployed in an
177 augmented randomized complete block design (ARCBD) (Crossa and Federer, 2012)
178 with c = 3 checks (random plants of the parents BGDJ, WAT and the F_1 hybrid
179 BGDJxWAT), r= 10 blocks extending in rows. Because the number of entries was not a
180 multiple of the number of blocks, nine blocks had 13 entries and the 10th block had 8
181 entries. Nine traits were ultimately evaluated in 121 live coconut trees: Number of
182 Leaves (NL), Height of Second Leaf Hem (cm) (HSLH), Petiole Length (cm) (PL), Rachis
183 Length (cm) (RL), Petiole Width (cm) (PW), Petiole Thickness (cm) (PT), emergence of

184 the base of the stipe (BOLE), Number of Bunches with fruits (NBF) and Days to Launch
185 of the First Spathe (DLFS). BOLE was recorded in a binary fashion with presence of bole
186 when it extended at least 70 cm from the ground, and absence when at less than 70
187 cm from the ground. DLFS was used as a direct quantitative measure of time to
188 flowering. These traits, but BOLE, are typically used to differentiate dwarf from tall
189 plants in the early stages of life. Measurements were taken according to the
190 standardized methods described by Santos et al. (1996). Trait evaluations were carried
191 out at one and two years after planting, on June 30, 2019 and July 30, 2020 with
192 evaluation of morphological leaf traits. Flowering initiation was measured on each
193 individual plant according to the emergence of the first spathe starting on October 11,
194 2020 and then by a monthly monitoring to precisely catch the launch of the first
195 spathe. The number of days for the emergence and opening of the subsequent spathes
196 until the tenth spathe was recorded until the least evaluation on August 11, 2022. The
197 final evaluations of the morphological traits were carried out on May 10, 2022, with
198 the exception of NBF, which was evaluated on August 11, 2022. Pearson correlations
199 were estimated to assess the correlation between traits using the Corrplot package
200 available in R (Wei et al., 2021). Phenotypic data for all traits but BOLE was analyzed
201 with the following mixed model: $Y_{ij} = \mu + B_i + E_j + C(_i)_j + e_{ij}$ where Y is the observed
202 phenotypic value of the genotype entry (j) in block (i), μ is the overall mean, B is the
203 fixed block effect, E is the random genotype entry effect, C is the random effect of the
204 common checks in blocks and e is the random residual effect. Best linear unbiased
205 predictors (BLUPs) were estimated using the software SELEGEN (Resende, 2016) under
206 model 76 (augmented blocks, genotypes, one plant per plot, single location, fixed
207 check).

208 ## 2.4 Linkage map construction

209 The raw SNP calls were filtered for quality for the linkage mapping analyses.
210 The first filtering step was based on a call rate >0.95 followed by selection of SNP
211 markers that fit the expected segregation proportions in an F_2, by a Chi-square test
212 under the null hypothesis of a 1:2:1 segregation ratio with a slightly more relaxed
213 threshold (α>0.001) to allow including SNPs even with some level of segregation
214 distortion given the particularity of the mapping population. Linkage analysis and
215 construction of the genetic map were performed according to the standard F_2 model
216 using JoinMap v3.0 (Van Ooijen and Voorrips, 2001). The genotypes of the F_2
217 population were coded, according to the format <hkxhk> for an unknown linkage
218 phase configuration and three possible genotypic classes. Markers were assigned to
219 linkage groups (LG) via the clustering module with LOD (logarithm of the odds) scores
220 greater than 15, maximum recombination fraction of 0.4, under a Kosambi mapping
221 function. Linkage maps were drawn and aligned to the assembled genomes using
222 MAPCHART (Voorrips, 2002). For the alignments, recombination distances were
223 expressed in centiMorgans and physical distances in Mbp.

224 ## 2.5 Marey maps and recombination rates in the genome of
225 ## *Cocos nucifera*

226 To estimate local recombination rates across the 16 coconut chromosomes, the
227 69 base pair DArTseq sequences corresponding to the SNP markers were aligned to the
228 two existing chromosome-level coconut genome assemblies of Hainan Tall coconut: (1)
229 a draft assembly built using exclusively short Illumina paired-end sequencing (Yang et

230 al., 2021) hereafter called the YANG genome and (2) a reference-grade assembled
231 genome using long Nanopore single-molecule sequencing and Hi-C technology (Wang
232 et al., 2021) hereafter called the WANG genome. The FASTA sequences of the
233 chromosome assemblies were downloaded from their respective repositories. The
234 YANG genome from GenBank BIOPROJECT PRJNA374600, and the WANG genome from
235 the Genome Warehouse in the National Genomics Data Center (Beijing Institute of
236 Genomics) accession number GWHBEBT00000000, BIOPROJECT PRJCA005463. The
237 DArTseq sequences were mapped to the sequences of the 16 coconut pseudo-
238 chromosomes using BLASTn for highly similar sequences (megablast) with a cutoff E-
239 value <1E-05. DArTSeq sequences that mapped to a unique location in both genome
240 versions were used in further analyses. The relationships between the genetic and
241 physical positions of the mapped SNPs were represented by the local slope of the
242 curve adjusted to the datapoints in MAREY maps (Chakravarti, 1991). Curves were
243 fitted to the data using locally weighted scatterplot smoothing (LOESS) polynomial
244 regression with a smoothing parameter of 0.3 using MareyMap Online (Siberchicot et
245 al., 2017). Sporadic abnormal points from the map that did not fit the expected
246 monotonously increasing relationship between physical and genetic positions were
247 removed using the available functionality in the software. The physically mapped
248 markers were used to obtain an estimate of the effective physical coverage achieved
249 by the genetic map and the recombination rates in cM/Mb along the chromosomes.
250 Pearson's correlations along windows of 1 Mb were calculated between the average
251 recombination rate in the 1 Mb interval and the number of genes as annotated in the
252 coconut chromosomes in the YANG genome (Yang et al., 2021).

253 ## 2.6 QTL mapping

254 QTLs detection was performed using the BLUPs for eight traits and the binary
255 0/1 value for BOLE with R/qtl version 3.5.3, using three different methods: interval
256 mapping (IM), Haley Knott regression (HK) and non-parametric interval mapping (Non-
257 parametric IM) for those traits that violated the assumption of normality (Broman et
258 al., 2003). The probability of genotype error (error.prob = 0.01) was calculated and the
259 threshold LOD score for QTL detection was determined by genome-wide LOD
260 significance thresholds, setting LOD thresholds at different alpha levels (α = 0.01; 0.05
261 and 0.1) using 1900 permutations to allow for the declaration of QTLs with variable
262 stringency levels in order to control also for Type II errors.

263 ## 2.7 Co-localization of the FLOWERING LOCUS T (FT) gene with
264 ## the flowering time QTL

265 A set of 198 expressed gene sequences in coconut were recently identified as
266 homologues of flowering-time genes in *Arabidopsis*. Five of them, annotated as FT
267 homologs to the *Arabidopsis thaliana* FT gene (AT1G65480) were found to be
268 differentially expressed between seedling and reproductive leaf samples in both tall
269 and dwarf coconut. Alternative splicing analysis showed that the FT gene produces
270 different transcripts in tall compared to dwarf coconut (Xia et al., 2020). We took all
271 the 87 *Arabidopsis thaliana* genes present in the annotation of the 198 coconut
272 expressed genes and aligned them to the QTL region on the corresponding
273 chromosomes assembled in the two genome assemblies using BLASTn specifically in

274 the genome stretch from 65 Mbp to 75 Mbp where the major effect QTL was mapped
275 (see below).

276 3. Results

277 3.1 SNP markers and linkage mapping

278 Genotyping by sequencing using DArTseq generated 86,719 raw SNP calls based
279 on the standard parameters used in DArTsoft. After applying a call rate threshold of
280 95% and a test for adherence to a null hypothesis of 1:2:1 segregation, 3,714 SNPs
281 (4.28% of the raw SNP calls) were retained for further linkage analyses (File S1).
282 Dominant presence/absence in silico DArTseq variants were not used due to their low
283 information content and considering that an adequate number of co-dominant
284 informative SNPs was already available for linkage mapping purposes. A linkage map
285 was ultimately built with 182 F_2 individuals that correspond to 364 meiotic events
286 sampled in the gametes from the recombined F_1 parents. All 3,714 SNPs were mapped
287 with LOD ≥15 and maximum recombination fraction of 0.4, in 16 linkage groups
288 matching the expected 16 coconut chromosomes. However, for the subsequent
289 assessment of the recombination rates and QTL mapping, only the SNPs that were
290 physically positioned on the genome assemblies (see below) were ultimately
291 considered on the linkage map (File S2). Linkage group numbering used for our map
292 was based on the physical positioning of SNP markers on the YANG genome
293 chromosomes which was published first in the literature. The chromosome numbering
294 used in the WANG genome was different but the correspondence was established and
295 reported throughout (Table 1). An average of 184.5 SNPs were mapped to each

296 chromosome, varying from a maximum of 329 SNPs on chromosome 1 to a minimum
297 of 101 SNPs on chromosome 15. The genetic map spanned a total of 2,124.3 cM in
298 recombination size, with an average linkage map length of 132.8 cM, and an average
299 intermarker recombination distance between adjacent marker pairs of 0.742 cM.
300 Chromosome 15 displayed a large recombination gap of 31.2 cM between two denser
301 linkage clusters although still linked by the minimum LOD 15 score threshold adopted
302 (Figure 1). Except for this large gap observed on chromosome 15, maximum
303 intermarker distance was 6.7 cM on chromosome 7.

304 3.2 Alignment of the linkage map to the genome assembly

305 The 3,714 DArTseq sequences containing the linkage mapped SNPs were
306 submitted to BLASTn against the chromosome assemblies. On the YANG genome out
307 of the 3,714 linkage mapped DArTSeq SNPs, 2,952 DArTSeq sequences were mapped
308 to unique locations with E-values <7.3e-05. The sequences for the remaining SNPs
309 either aligned to multiple locations or did not align to the assembled coconut
310 chromosomes and were removed from further analyses. On the WANG genome 3,027
311 DArTSeq sequences were mapped to unique locations with E-values <3.6e-11 (File S3).
312 On the YANG genome, the linkage map covered 1,035 Mb corresponding to a coverage
313 of approximately 43.14% of the 2,400 Mb *Cocos nucifera* Tall cultivar genome (Wang et
314 al., 2021). On the WANG genome, the linkage mapped SNPs covered a total of 2,382
315 Mb, a 99.27% coverage, more than twice the coverage obtained on the YANG genome
316 with a corresponding lower density of mapped SNPs and long stretches with no
317 segregating SNPs mapped to them. The average estimated physical inter SNP distance

318 were 349kb and 779kb, SNP density of 2.85 and 1.27 SNPs/Mb and maximum physical
319 distances of 9.7 and 63.4 Mb respectively on the YANG and WANG genomes (Table 1).

320 3.3 Marey maps and recombination rates

321 The linkage maps alignment to the 16 pseudochromosomes was largely colinear
322 with the physical assembly, with only sporadic inconsistencies of the map versus
323 genome positions, 2 in the YANG genome and 20 in the WANG genome (Figure 1; File
324 S4). As expected, on all linkage groups the alignment to the physically larger WANG
325 genome showed long sections of genome sequence with few or no SNP markers
326 mapped. The Marey maps showed plateaus of restricted recombination, where the
327 recombination distance does not follow the increase in physical distance along the
328 chromosome (Figure 2). These plateaus spanned considerably longer stretches for the
329 Marey maps on the WANG genome. From the Marey maps data, estimates of local
330 recombination rate were obtained for both genomes using LOESS (Locally Weighted
331 Scatterplot Smoothing) (File S4) and plotted for the YANG genome (Figure 2). Following
332 LOESS treatment of the data, the average local recombination rates were similar: 2.78
333 cM/Mb for the YANG genome and 2.32 cM/Mb for the WANG genome. The smoother
334 recombination rate curves closely followed expectations. Chromosomal segments of
335 restricted recombination in the Marey maps coincided with local valleys of low
336 recombination rate notably spotted on YANG chromosomes 1, 4, 5, 11 and 14, for
337 example and more accentuated on the corresponding WANG chromosomes.

338 Average recombination rates per chromosomes varied across chromosomes up
339 to more than twofold (e.g., 1.98 cM/Mb on chromosome 3 and 5.18 cm/Mb on
340 chromosome 15 on the YANG genome). However, the correlation between the rates

341 estimated on the two genome versions was high and significant (r = 0.85; p-value = 3E-
342 5). The highest rate on chromosome 15 is likely the result of the large linkage gap
343 observed on this chromosome. The average recombination rate across the entire
344 genome were similar, at 2.79 and 2.32 cM/Mb for the two genomes (Table 1).
345 Furthermore, taking advantage of the gene annotation provided for the YANG genome
346 sequence, we underlaid the frequency distribution of the number of genes in 1 Mb
347 intervals, equivalent to gene density, to the smoothed recombination rate curve in the
348 same 1 Mb segment (Figure 2). Visually an almost perfect direct relationship was seen
349 between gene density and recombination rate. This visual relationship was further
350 validated by observing high and significant Pearson correlation between average
351 recombination rate and number of genes in the 1 Mb intervals estimated for the YANG
352 genome. For all chromosomes but chromosomes 7 and 15 these correlations were high
353 and significant (p-value <0.001) (Table 1) suggesting, once again, some different
354 behavior as far as recombination for these two chromosomes.

355 3.4 Trait variation and correlations

356 The F_2 individuals displayed extensive segregation for all traits measured, as
357 expected in a recombinant F_2 population of divergent cultivars. Raw phenotypic values
358 and BLUPs are provided in File S5. The continuous traits showed an approximately
359 normal distribution, although with some skewness, most notably for NBF and DLFS
360 (Figure 3). BOLE expression fit a 3:1 segregation ratio with 98 plants showing no bole
361 and 23 with bole (Chi-square 2.31; p-value = 0.128). Days to Launch of the First Spathe
362 (DLFS) varied from a minimum of 812 days for the precocious flowering plants to a
363 maximum of 1608 days for the late blooming ones with an average of 1287 ± 214.5

364 days. One plant therefore displayed 2.2 standard deviations below the mean and 13
365 flowered with less than 1000 days, corresponding to more than one standard deviation
366 below the mean. Eight of these very early flowering plants displayed the highest
367 numbers (≥13) fruit per bunch (NBF). Significant negative correlations were seen
368 between DLFS and NL, HSLH, BOLE and NBF, and a significant positive correlation with
369 PL (Figure 4). Positive significant correlations were seen between five of the six leaf
370 morphology traits (NL, HSHL, RL, PW and PT), except PL that showed no correlation
371 with all other five traits. Positive and significant correlations were also observed
372 between NBF and NL, HSLH, RL and BOLE. Coconut trees with a recorded bole flowered
373 on average after 1098 days and produced an average of 9.5 fruit per bunch while
374 plants without bole flowered on average after 1347 days, and produced 5.96 fruit per
375 bunch.

376 3.5 Mapping and haplotype analysis of a major flowering time 377 QTL

378 QTL detection was carried out with three methods, IM, CIM and HK to assess
379 consistency of results and minimize type I errors. Significant QTL peaks were declared
380 based on the LOD limit analysis for the different alpha levels to allow the detection of
381 suggestive QTLs in order to minimize Type II errors. The significance thresholds
382 indicated LOD limits of 4.15, 4.49 and 5.22 respectively for the different alpha levels (α
383 = 0.01; 0.05 and 0.1) (Table 2). Results with CIM showed a considerably larger number
384 of 16 putatively significant QTLs in 11 chromosomes when compared to the results
385 with IM and HK. These CIM results are not discussed further but are provided (File S6).
386 Genome-wide QTL profile results across the 16 chromosomes obtained with the three

387 QTL detection methods, for the four traits for which significant QTLs were detected are
388 provided for a full visualization of results. The LOD limit thresholds are specified by the
389 differentially dotted lines (Figure 5).

390 Overall, consistent QTLs across the methods were detected on chromosome 3
391 for DFLS, BOLE and PL and on chromosome 1 for NBF. A genomic segment at the tip of
392 chromosome 3 spanning 52 significantly linked SNPs to DFLS stands out as a major
393 effect QTL for flowering time, explaining an estimated 64% of the variation in DLFS.
394 The alignment of the linkage map to the chromosome 3 of the YANG genome and
395 chromosome 4 of the WANG genome allowed a detailed haplotype analysis of this
396 segment. In the YANG genome starts at SNP 100285601_C>G-14 with LOD 4.99 located
397 at 117.99 cM corresponding to 68.84 Mbp, and ends at SNP 100270789_A>G-59 with
398 LOD 6.53 located at 148.17 cM corresponding to position 82.32 Mbp (File S3). In the
399 WANG genome it spans 55 SNPs including the 52 mapped to the YANG genome form
400 position 162.7 Mb to the end of the chromosome at 178.5 Mb. Within this segment,
401 the highest QTL peak (LOD 11.86) is located at SNP 100226499_C>T-34, positioned at
402 129.11 cM and 73.15 Mbp, flanked by SNPs 100287206_T>A-55 and 100273632_T>G-
403 15. At SNP 100226499_C>T the T allele inherited from the Dwarf parent AVeBrJ causes
404 a major reduction in the time to flower, suggesting incomplete dominance of the locus.
405 Heterozygous genotype G/T confers a reduction from 1460 to 1390 days to the launch
406 of the first spathe, while the homozygous T/T genotype confers a further reduction of
407 almost 300 days, as the coconut trees bearing this genotype flowered on average after
408 1110 days (Figure 6). In addition to acting on early flowering, the same genomic
409 segment is involved in the control of BOLE and PL. The LOD peak for both QTLs for
410 BOLE and PL was located at the same SNP 100228320_G>A-40, at 132.62 cM and

411 75.61 Mbp. The co-localization of QTLs for three traits suggests a pleiotropic action of
412 this major effect QTL segment on chromosome 3. Some additional suggestive QTLs
413 were detected for PL on chromosomes 1, 2, 4, 6 that were significant at α = 0.1 based
414 on the IM analysis but that did not reach significance with the two other QTL detection
415 methods. Finally, a single QTL was also found for NBF on chromosome 1 whose Dwarf
416 allele confers an increase in the number of fruits per bunch.

417 3.6 Co-localization of the flowering time QTL with the 418 FLOWERING LOCUS T (FT)

419 Out of the 87 *Arabidopsis thaliana* genes involved in flowering-time pathways
420 that were found to be homologous to 198 coconut genes (Xia et al., 2020), only the
421 complete coding sequence of the *Arabidopsis thaliana* putative flowering signals
422 mediating protein FT (At1g65480) produced strongly significant alignment to the
423 flowering time QTL mapped on linkage group 3. The FT gene (At1g65480) complete cds
424 mRNA (accession AY065378.1) with 840 bp produced two hits in the YANG genome: (i)
425 at 70,554,038 to 70,554,249 bp with bit score 108, 71% identity, e-value = 3e-23 and
426 0/212 gaps (0%) and (ii) at 73,265,231 to 73,265,450 bp with bit score 88.7, 70%
427 identity, e-value = 3e-17 and 3/222 (1%) gaps (Figure 6; File S7). These hits are located
428 respectively at 137 kb from SNP 100241292_A>G-33 LOD 9.55 and 117 kb from SNP
429 100226499_C>T-34 this last one had the highest LOD score (LOD 11.86) in the QTL
430 region. When the FT gene (At1g65480) was blasted against the corresponding
431 chromosome 4 in the WANG genome it also produced two significant hits at 164.688
432 Mb (e-value = 7E-21) and 168.065 Mb (e-value = 7E-15) that correspond to the
433 genomic positions at the tip of the chromosome (Figure 1; File S8), further

434 corroborating the finding. This co-localization result between the flowering time QTL
435 and the FLOWERING LOCUS T (FT) gene when taken together with the splice variant
436 analysis reported earlier (Xia et al., 2020), strongly suggests that the underlying
437 candidate gene to the flowering time QTL mapped in this study could be an FT
438 homolog in *Cocos nucifera.*

439

440 # 4. Discussion

441 We have carried out QTL mapping in *Cocos nucifera* based on a novel mapping
442 approach for the crop, using an outbred F_2 population derived from open pollination
443 intercrossing of F_1 hybrids. With this approach we were able to segregate and track the
444 variation contributed by the inbred Dwarf in the F_2 by selecting SNP markers fixed for
445 alternative alleles between the Brazilian Green Dwarf from Jiqui (BGDJ) and the West
446 African Tall (WAT) cultivar segregating in a bona fide F_2 configuration despite the
447 outbred nature of the population. Almost 3,000 SNPs obtained by genotyping by
448 sequencing were positioned on the two existing chromosome-level coconut genome
449 assemblies. By aligning the linkage map to the genome sequences, we provided an
450 independent assessment of the contiguity of the current coconut reference genomes,
451 and a detailed analysis of the relationship between recombination rate and physical
452 distance for the corresponding coconut chromosomes. Furthermore, based on the
453 segregation observed for traits related to precocious behavior inherited from the
454 Dwarf cultivar, we mapped a major effect QTL for flowering time on chromosome 3.
455 Flowering Locus T (FT) gene homologs of coconut, previously described as involved in
456 flowering time by alternative splice variant analysis, were co-localized with the

457 molecular phenotype mapped QTL, providing evidence for its role as the putative
458 underlying gene.

459 4.1 Exploiting the unique genetics of the Tall x Dwarf coconut 460 hybrid for linkage mapping in an outbred F_2.

461 The linkage map reported in our study is the first one in coconut built from an
462 F_2 segregating population from a Tall x Dwarf hybrid. Previous maps either used hybrid
463 F_1 or backcross (BC1) populations (Herrán et al., 2000; Ritter et al., 2000; Lebrun et al.,
464 2001; Yang et al., 2021) or a cross between Tall cultivars (Riedel et al., 2009).
465 Differently from a conventional F_2 populations generated by selfing an individual F_1
466 plant, the particular genetics of coconut allowed using an open pollinated progeny of
467 an F_1 hybrid field. The parental F_1 plants composed a commercial production
468 plantation with seeds resulting from controlled pollination between a pollen mix of
469 several Tall coconut parents on female flowers of several Dwarf plants. In the
470 particular case of coconut, we took advantage of the fact that the Dwarf variety is
471 essentially a fixed inbred line with very little if any residual heterozygosity, while the
472 Tall parents are allogamous, heterozygous and genetically diverse (Santos et al., 2020;
473 Wang et al., 2021; Muñoz-Pérez et al., 2022). The F_1 plants SNP genotypes would
474 potentially differ only in what was inherited from the Tall parents, but SNP markers
475 fixed in the Tall variety and polymorphic in relation to the Dwarf would segregate in a
476 1:2:1 ratio in the F_2, irrespective of what Tall parent generated each different F_1 plant
477 which in turn were intercrossed to produce the F_2 population. This premise proved
478 valid, and 3,714 SNPs called with a call rate >95%, fit the expected segregation and
479 were linkage mapped. This SNP selection strategy essentially converted the outbred F_2

480 population into a standard F_2, allowing the appropriate application of linkage and QTL
481 mapping. Approximately 20% of the sequences of linkage mapped DArTSeq mapped
482 to multiple locations in the two genomes and were left out of subsequent analysis, as
483 no objective criteria allowed choosing one location over another. Therefore, for QTL
484 mapping analyses we used only around 3,000 linkage mapped SNPs that could be
485 anchored to unique positions on the 16 assembled chromosomes of the two genome
486 versions.

487 The linkage map assembled in the 16 expected linkage groups spanned a total
488 of 2,124.3 cM, slightly smaller than the linkage map reported earlier by Yang et al.
489 (Yang et al., 2021) with 2,365 cM built from a backcross (BC_1) population with 216
490 individuals and 8,402 SNPs retained with >80% call rate. Linkage group recombination
491 sizes of our map were also similar to those reported by Yang et al. in the BC_1 map
492 (Spearman rank correlation 0.72), including the only large recombination gap in
493 chromosome 15, starting at around the 40 cM position (Figure 1). This recombination
494 gap was hypothesized to be due to reduced heterozygosity resulting from a selection
495 sweep in favor of the allele transmitted from the Dwarf parent observed in the YANG
496 genome assembly (Yang et al., 2021).

497 Although our map was built from a smaller number of individuals than the BC_1
498 map used to anchor the YANG genome (Yang et al., 2021), those were derived from
499 two recombined gametes from the F_1 parents, therefore sampling twice as many
500 meiotic events as in a BC1 population. The number of recombination events per
501 meiosis captured in the mapping population is one of the main drivers of mapping
502 accuracy, with an F_2 being the most efficient configuration (Liu, 1998; Ferreira et al.,

503 2006). Additionally, for improved linkage map quality, we decided to use only SNPs
504 with call rate >95% aware of the potential reproducibility challenges of marker data
505 derived from genotyping by sequencing methods in heterozygous genomes (Myles et
506 al., 2010). From the raw data, 10,576 DArTSeq markers were retained at >95% call
507 rate, and the main detractor of the final SNPs number was the test for the 1:2:1
508 segregation. This substantiates the variability in the F_1 parents contributed by the Tall
509 grandparental pollen pool. This observation indicates that a self-pollinated progeny
510 from a single F_1 plant would possibly allow mapping a considerably larger number of
511 DArTSeq SNP markers.

512 4.2 The F_2 linkage map provides an independent assessment of
513 the properties of the coconut genome assemblies

514 The DArTseq method using the rare cutter SbfI combined to the frequent MseI
515 enzyme proved effective for complexity reduction and enrichment of the sequenced
516 pool for low copy genomic regions across most of the large coconut genome,
517 generating a large number of segregating markers (Sansaloni et al., 2011). Our
518 mapping and data quality control approach proved effective to order SNPs markers
519 along the linkage groups into robust maps, highly colinear with the genome sequences
520 (Table 1). The physical distance covered by our F_2 linkage map was 1035.4 Mb on the
521 YANG genome, slightly higher than the 1,020 Mb of the Yang et al. BC_1 map, while on
522 the WANG genome, the mapped SNPs covered 2,382 Mb, reaching a 99.27% coverage.
523 As expected, very few segregating DArTSeq sequences and the corresponding SNPs
524 were mapped to long physical stretches covering several hundred Mb of DNA of the
525 reference-grade WANG genome assembly produced by nanopore long read

526 sequencing (Figure 1). These regions were not sampled in the YANG genome,
527 assembled exclusively with short read sequencing. The extensive genome gaps with no
528 mapped SNPs and low gene density (Figure 2), likely correspond to heterochromatin,
529 typically found at centromeres and telomeres, known to be relatively gene poor,
530 mostly consisting of repetitive DNA sequences (Allshire and Madhani, 2018), where the
531 DArTSeq method by principle tends not to sample restriction fragments. Performing
532 linkage mapping in those heterochromatic regions will prove challenging, requiring
533 approaches that can target the occasional low-copy regions scattered in the repetitive
534 DNA. Using a selfed F_1 progeny might prove valuable in this respect to sample much
535 larger number of segregating DArTSeq SNPs, possibly targeting low-copy interspersed
536 segments in these heterochromatic regions of the coconut genome.

537 The alignment of the linkage maps to the genome assembly indicated
538 consistent ordering between the Joinmap estimated positions of the SNPs, and their
539 relative physical order along the assembled chromosomes, with only sporadic
540 inconsistencies seen most notably at the tip of some chromosomes (Figure 1). These
541 localized inconsistencies could be due either to erroneous linkage map ordering or
542 misassembled genome scaffolds. Historically, the majority of the inconsistencies
543 between the physical and genetic map order pointed to errors in the physical map
544 order (DeWan et al., 2002), making linkage maps effective tools to correct genome
545 assemblies (Fierst, 2015). However, sequencing technologies and assembly algorithms
546 have improved tremendously in recent years. The alignment of the linkage map to two
547 independent genome assemblies, one of them built with long reads, indicates that
548 those few SNPs that show inconsistent positions in relation to both genome

549 assemblies, for example at the tips of chromosomes 8, 9 and 12, most likely were
550 inaccurately mapped.

551 The largely consistent genetic to physical position of the mapped SNPs led us to
552 carry out further analysis of this relationship for each coconut chromosome by
553 estimating local recombination rates in cM/Mb, given by the slope of the curve built
554 with graphical Marey maps. Additionally, the gene density histogram distribution
555 annotated in the YANG genome was merged to the Marey maps for a combined view
556 (Figure 2). In all chromosomes, the Marey maps showed genomic stretches of
557 constrained recombination, where the recombination distance does not follow the
558 linear increase in physical distance and gene density drops. This observation was
559 evidently more distinct in the WANG genome Marey maps that included the
560 heterochromatic regions of the genome. These regions are typically considered to be
561 the putative location of centromeres. Considering the WANG chromosome numbering
562 for now, these were located more toward the extremes of the chromosome
563 (chromosomes 3, 7, 8, 9, 10, 12, 13 and 16) that would correspond to acrocentric or
564 even telocentric chromosomes. In the other chromosomes these regions are found
565 more toward the middle (Figure 2). Centromeres are essential for faithful segregation
566 of chromosomes both in mitosis and meiosis and are typically rich in repetitive
567 sequences in many eukaryotes (Achrem et al., 2020). Equivalent observations to ours
568 on the putative centromere positions was reported in the YANG genome (Yang et al.,
569 2021), establishing their correlation to the presence of repetitive rich DNA regions that
570 were challenging to assemble. A few localized negative recombination rate estimates
571 were also observed when the LOESS curve under passed the red dotted line, for
572 example on chromosomes 7, 8, 9 and 12 (Figure 2). These localized negative estimates

573 coincide with the inconsistent genetic to physical map alignments as described above
574 and are usually located at the tip of chromosomes. All our results taken together, on
575 the collinearity between our linkage map and both physical genomes provide an
576 independent experimental validation of the genome assemblies currently available for
577 coconut and establish the correspondence of chromosome numbering used in the two
578 reports (Figure 2).

579 4.3 Colocation of a major effect QTL with the FLOWERING 580 LOCUS T (FT) provides evidence for its role in early flowering

581 Little is known about the underlying mechanisms of early flowering in dwarf
582 coconut. Knowledge on the complex physiology and genetics of flowering initiation has
583 come mainly from annual plants including the model species *Arabidopsis* as well as
584 crop plants, which typically flower and set seeds within a single year (Komeda, 2004;
585 Roux et al., 2006). Less is known about flowering time in perennial plants which
586 typically have distinguishable transition from a juvenile to an adult phase, the
587 developmental stage that determines the emergence of flower meristems. It is now
588 well established, however, that the formation of flower structures is largely conserved
589 across flowering plants, annual and perennial, with relatively minor variations in the
590 role of key developmental genes (Khan et al., 2014). Amongst the several genes
591 identified as involved in regulation of flowering time, the expression of FLOWERING
592 LOCUS T (FT) and its homologues has been shown to accelerate the onset of flowering
593 in a number of plant species (Putterill and Varkonyi-Gasic, 2016). During the course of
594 our study, we came across a transcriptomics report in coconut showing that the
595 *FLOWERING LOCUS T* (FT) gene generates different transcripts in tall compared to

596 dwarf coconut, with the shorter splice variant of FT present exclusively in dwarf
597 varieties but absent in most tall coconuts (Xia et al., 2020). The authors suggested that
598 this FT splice variant could be the putative causal mechanism for flowering time
599 differentiation between the dwarf and tall coconut types, although they recommended
600 further investigation and validation to confirm this effect. By collocating a phenotype-
601 derived major QTL, detected agnostically to any prior gene-centered hypothesis, our
602 study provides independent validation of the FT gene as the underlying major
603 functional variants controlling flowering time between the two coconut varieties.

604 4.4 The *FT* locus likely controls other precocity traits in Dwarf 605 coconut

606 A number of traits were targeted in previous QTL mapping studies in coconut,
607 such as yield, fruit components, early germination and cuticular wax (Herrán et al.,
608 2000; Ritter et al., 2000; Lebrun et al., 2001; Baudouin et al., 2006; Riedel et al., 2009).
609 Flowering time, however could not be approached because it did not segregate in
610 intermediate F_1 hybrid families and less so in progeny of crosses between Tall cultivars.
611 Two studies to date have reported on the patterns of genetic variation in F_2
612 populations of coconut hybrids, although without attempting QTL mapping. Ample
613 segregation was reported for a number of vegetative and morphological flowering
614 traits, including height growth and the presence of a bole, for which the presence of at
615 least one major gene each, with incomplete dominance was suggested (Namboothiri
616 et al., 2011; Perera et al., 2016). Curiously, despite its importance as a trait directly
617 linked to production, time to flower was not assessed. Our study is therefore the first
618 one to tackle flowering time in coconut by a QTL mapping approach facilitated by the

619 strong segregation seen in the F_2. In our experiment we could not, however, measure
620 height growth with confidence and include this trait in the mapping work. Recently a
621 GWAS was carried out in a collection of Tall and Dwarf cultivars identifying a major
622 effect QTL for height growth (Wang et al., 2021). The leading SNP for the GWAS hit was
623 mapped to WANG chromosome 12, co-located in the promoter region of the
624 gibberellin (GA) biosynthetic enzymes GA 20-oxidases (GA20ox) further backed by
625 expression analysis, validating previous reports (Boonkaew et al., 2018). These results
626 strongly support the role of GA20ox in controlling height growth difference between
627 Tall and Dwarf coconuts. Taken together with the detection of a major flowering time
628 QTL on chromosome 4 of WANG genome (chromosome 3 of YANG) (Figs 5 and 6) and
629 its colocation with the FT gene, these results also suggest that height growth and
630 flowering time in coconut involve different major effect loci in line with the early
631 proposal of two independent major loci (Perera et al., 2016) , although it cannot be
632 ruled out that the FT gene is also involved in height growth (see below).

633 Petiole length (PL) and the presence of a bole (BOLE) were also assessed in our
634 study. Both traits are typically used as morphological markers to identify dwarf plants
635 (Batugal et al., 2009). In fact, PL and BOLE showed significant direct (0.466) and inverse
636 (-0.502) correlation with flowering time (DLFS) (Figure 4). Major effect QTLs were also
637 detected for these traits in the same exact region on chromosome 3 suggesting that
638 the *FT* gene might also be affecting these traits (Figure 5). The *FT/TFL1* gene family has
639 been extensively studied in flowering plants. It constitutes a major target of evolution
640 in nature, as a single essential gene that has played a central role in plant
641 diversification and adaptation (Pin and Nilsson, 2012). FT homologs have been
642 identified in many species, demonstrating general conservation of functions across

643 gymnosperms and angiosperms. It encodes a major florigen, a key flowering hormone
644 in controlling flowering time. Studies in a number of species have revealed diverse
645 roles of the FT/TFL1 gene family in plant developmental processes other than
646 flowering regulation, with a distinct effect on stem and leaf development, mainly in
647 the inhibition of stem and leaf growth (Wickland and Hanzawa, 2015; Freytes et al.,
648 2021). It is therefore plausible that *FT* is directly affecting PL and the formation of a
649 bole structure in coconut as well.

650 5. Conclusions: implications for coconut advanced breeding 651 lines

652 From the conventional coconut breeding perspective, offspring of F_1 hybrids
653 would in principle not be desirable for commercial production due to the wide
654 variation in yield traits among F_2 coconut trees. Nevertheless, the two previous studies
655 of F_2 populations have reported individuals displaying high husked nut weights,
656 indicating little or no inbreeding depression, likely resulting from the inbred nature of
657 the ancestral Dwarf grandparent. These results indicated good potential of extracting
658 recombined lines from F_2 populations with desirable characters (Fernando and Perera,
659 1997; Namboothiri et al., 2011). Still, no developments have been made to implement
660 this breeding strategy in coconut possibly due to the long time necessary to develop
661 and eventually propagate such recombined lines.

662 The results of our study open a fundamentally new perspective in terms of
663 marker assisted selection (MAS) in coconut breeding. Knowledge of the position and
664 the genotypes at the SNP markers linked to the flowering time QTL would easily allow

665 selecting hybrid F_2 plants homozygous for the early flowering haplotype. Homozygosity
666 for the favorable alleles at SNPs 100226499_C>T-34, 100287206_T>A-55 and
667 100273632_T>G-15, inherited from the Dwarf parent BGDJ caused a reduction in the
668 time to flower around 400 days in our experiment. Our data also showed a significant
669 negative correlation between the necessary days to flowering (DLFS) and NBF (Figure
670 4). Early flowering plants displayed some of the highest numbers of fruit per bunch and
671 a separate QTL was mapped in chromosome 1 which could be selected by a set of
672 linked SNPs flanking the lead SNP 100237259_A>G-48 (Table 2). This small set of SNPs
673 could be used for high throughput inexpensive MAS screening of F_2 plants at ultra-
674 early stages of development or even at the embryo stage. Juvenile tissue of these
675 selected individuals could be induced to somatic embryogenesis (Pérez-Núñez et al.,
676 2006) or, more successfully, to shoot culture (Wilms et al., 2021) for clonal
677 propagation. This would capture the full genetic value of these plants allowing
678 regenerating thousands of plants indefinitely, providing the coconut industry with a
679 solution for their current need of homogeneous quality planting material.

680 Data availability statement

681 All genotypic and phenotypic data are included in the Supplementary Material. Further
682 inquiries can be directed to the corresponding author.

683 Author contributions

684 DG, WBSA and CAPP contributed to conception and design of the study. CAPP
685 performed the field experimental work. WBSA carried out data analysis with input and

help from DG. DG wrote the manuscript and all co-authors subsequently contributed to it by editing the final version.

Funding

This work was partially supported by EMBRAPA and by FAP-DF (Fundação de Apoio à Pesquisa do Distrito Federal) through grants RECGENOMICS 00193- 00000924/2021-92 and NEXTREE 0193.001.198/2016; WBSA had a doctoral grant and DG a productivity fellowship from CNPq. There was no additional external funding received for this study and the funders had no role in study design, data collection and analysis, decision to publish, or preparation of the manuscript.

Acknowledgments

We would like thank the entire staff of field technicians EMBRAPA Tabuleiros Costeiros who were involved in establishing and managing the several field trials, and collecting and organizing the data used in this study. We thank Dr. Orzenil B. Silva-Junior and Dr. Roberto Togawa for assistance with the BLAST analysis against the YANG and Wang et al. genomes respectively.

Institutional Review Board Statement: Not applicable.

Informed Consent Statement: Not applicable.

Conflicts of Interest: The authors declare that the research was conducted in the absence of any commercial or financial relationships that could be construed as a potential conflict of interest.

References

Achrem, M., Szucko, I., and Kalinka, A. (2020). The epigenetic regulation of centromeres and telomeres in plants and animals. *Comparative Cytogenetics* 14**,** 265-311. https://doi.org/10.3897/CompCytogen.v14i2.51895

Allshire, R.C., and Madhani, H.D. (2018). Ten principles of heterochromatin formation and function. *Nature Reviews Molecular Cell Biology* 19**,** 229-244. https://doi.org/10.1038/nrm.2017.119

Batugal, P., Bourdeix, R., and Baudouin, L. (2009). "Coconut Breeding," in *Breeding Plantation Tree Crops: Tropical Species,* eds. S.M. Jain & P.M. Priyadarshan. (New York, NY: Springer New York), 327-375. https://doi.org/10.1007/978-0-387-71201-7_10

Baudouin, L., Lebrun, P., Konan, J.L., Ritter, E., Berger, A., and Billotte, N. (2006). QTL analysis of fruit components in the progeny of a Rennell Island Tall coconut (Cocos nucifera L.) individual. *Theoretical and Applied Genetics* 112**,** 258-268. https://doi.org/10.1007/s00122-005-0123-z

Boonkaew, T., Mongkolsiriwatana, C., Vongvanrungruang, A., Srikulnath, K., and Peyachoknagul, S. (2018). Characterization of GA20ox genes in tall and dwarf types coconut (Cocos nucifera L.). *Genes & Genomics* 40**,** 735-745. https://doi.org/10.1007/s13258-018-0682-4

Broman, K.W., Wu, H., Sen, Ś., and Churchill, G.A. (2003). R/qtl: QTL mapping in experimental crosses. *Bioinformatics* 19**,** 889-890. https://doi.org/10.1093/bioinformatics/btg112 %J Bioinformatics

Chakravarti, A. (1991). A Graphical Representation of Genetic and Physical Maps - the Marey Map. *Genomics* 11**,** 219-222. https://doi.org/Doi 10.1016/0888-7543(91)90123-V

Crossa, J., and Federer, W. (2012). I.4 Screening Experimental Designs for Quantitative Trait Loci, Association Mapping, Genotype-by Environment Interaction, and Other Investigations. *Frontiers in Physiology* 3. https://www.frontiersin.org/articles/10.3389/fphys.2012.00156

Dewan, A.T., Parrado, A.R., Matise, T.C., and Leal, S.M. (2002). The Map Problem: A Comparison of Genetic and Sequence-Based Physical Maps. *The American Journal of Human Genetics* 70**,** 101-107. https://doi.org/https://doi.org/10.1086/324774

Fao (2021). "FAOSTAT statistical database". (http://www.fao.org/faostat/en/#data: Food and Agricultural Organization, Rome (Date accessed: March 10, 2022)). https://search.library.wisc.edu/catalog/999890171702121

Fernando, W.M.U., and Perera, P. (1997). Evaluation of genotypes arising from F2 generation segregations in dwarf × tall crosses of cocos nucifera. *Cord.* 13**,** 26-35. https://www.scopus.com/inward/record.uri?eid=2-s2.0-83155176911&partnerID=40&md5=56effca7eb012edcc68844ba61a1210e

Ferreira, A., Da Silva, M.F., Silva, L., and Cruz, C.D. (2006). Estimating the effects of population size and type on the accuracy of genetic maps. *Genetics and Molecular Biology* 29**,** 187-192. https://doi.org/10.1590/s1415-47572006000100033

Fierst, J.L. (2015). Using linkage maps to correct and scaffold de novo genome assemblies: methods, challenges, and computational tools. *Frontiers in Genetics* 6. https://doi.org/10.3389/fgene.2015.00220

Freytes, S.N., Canelo, M., and Cerdan, P.D. (2021). Regulation of Flowering Time: When and Where? *Current Opinion in Plant Biology* 63. https://doi.org/10.1016/j.pbi.2021.102049

Gunn, B.F., Baudouin, L., and Olsen, K.M. (2011). Independent Origins of Cultivated Coconut (Cocos nucifera L.) in the Old World Tropics. *Plos One* 6. https://doi.org/10.1371/journal.pone.0021143

Herrán, A., Estioko, L., Becker, D., Rodriguez, M.J.B., Rohde, W., and Ritter, E. (2000). Linkage mapping and QTL analysis in coconut (Cocos nucifera L.). *Theoretical and Applied Genetics* 101**,** 292-300. https://doi.org/10.1007/s001220051482

758 Inglis, P.W., Pappas, M.D.C.R., Resende, L.V., and Grattapaglia, D. (2018). Fast and inexpensive
759 protocols for consistent extraction of high quality DNA and RNA from challenging plant
760 and fungal samples for high-throughput SNP genotyping and sequencing applications.
761 *PLosOne* 13**,** e0206085. https://doi.org/10.1371/journal.pone.0206085
762 Khan, M.R.G., Ai, X.-Y., and Zhang, J.-Z. (2014). Genetic regulation of flowering time in annual
763 and perennial plants. *WIREs RNA* 5**,** 347-359.
764 https://doi.org/https://doi.org/10.1002/wrna.1215
765 Komeda, Y. (2004). GENETIC REGULATION OF TIME TO FLOWER IN ARABIDOPSIS THALIANA.
766 *Annual Review of Plant Biology* 55**,** 521-535.
767 https://doi.org/10.1146/annurev.arplant.55.031903.141644
768 Lebrun, P., Baudouin, L., Bourdeix, R., Konan, J.L., Barker, J.H.A., Aldam, C., Herran, A., and
769 Ritter, E. (2001). Construction of a linkage map of the Rennell Island Tall coconut type
770 (Cocos nucifera L.) and QTL analysis for yield characters. *Genome* 44**,** 962-970.
771 https://doi.org/10.1139/gen-44-6-962
772 Liu, H.B. (1998). *Statistical Genomics, Linkage, Mapping and QTL Analysis.* Boca Raton, Florida:
773 CRC.
774 Muñoz-Pérez, J.M., Cañas, G.P., López, L., and Arias, T. (2022). Genome-wide diversity analysis
775 to infer population structure and linkage disequilibrium among Colombian coconut
776 germplasm. *Scientific Reports* 12**,** 2958. https://doi.org/10.1038/s41598-022-07013-w
777 Myles, S., Chia, J.M., Hurwitz, B., Simon, C., Zhong, G.Y., Buckler, E., and Ware, D. (2010). Rapid
778 Genomic Characterization of the Genus Vitis. *Plos One* 5**,** e8219.
779 https://doi.org/10.1371/Journal.Pone.0008219
780 Namboothiri, C.G.N., Niral, V., Parthasarathy, V.A., and Muralidharan, K. (2011). Segregation,
781 phenotypic and genotypic variance and heritability in the F2 population of coconut
782 (*Cocos nucifera*). *Indian Journal of Agricultural Sciences* 81**,** 954-956.
783 Perera, L., Baudouin, L., and Mackay, I. (2016). SSR markers indicate a common origin of self-
784 pollinating dwarf coconut in South-East Asia under domestication. *Scientia*
785 *Horticulturae* 211**,** 255-262. https://doi.org/10.1016/j.scienta.2016.08.028
786 Pérez-Núñez, M.T., Chan, J.L., Sáenz, L., González, T., Verdeil, J.L., and Oropeza, C. (2006).
787 Improved somatic embryogenesis from Cocos nucifera (L.) plumule explants. *In Vitro*
788 *Cellular & Developmental Biology - Plant* 42**,** 37-43.
789 https://doi.org/10.1079/IVP2005722
790 Pin, P.A., and Nilsson, O. (2012). The multifaceted roles of FLOWERING LOCUS T in plant
791 development. *Plant, Cell & Environment* 35**,** 1742-1755.
792 https://doi.org/https://doi.org/10.1111/j.1365-3040.2012.02558.x
793 Putterill, J., and Varkonyi-Gasic, E. (2016). FT and florigen long-distance flowering control in
794 plants. *Current Opinion in Plant Biology* 33**,** 77-82.
795 https://doi.org/https://doi.org/10.1016/j.pbi.2016.06.008
796 Resende, M.D.V. (2016). Software Selegen-REML/BLUP: a useful tool for plant breeding. *Crop*
797 *Breeding and Applied Biotechnology* 16**,** 330-339. https://doi.org/10.1590/1984-
798 70332016v16n4a49
799 Riedel, M., Riederer, M., Becker, D., Herran, A., Kullaya, A., Arana-Lopez, G., Pena-Rodriguez,
800 L., Billotte, N., Sniady, V., Rohde, W., and Ritter, E. (2009). Cuticular wax composition
801 in Cocos nucifera L.: physicochemical analysis of wax components and mapping of
802 their QTLs onto the coconut molecular linkage map. *Tree Genetics & Genomes* 5**,** 53-
803 69. https://doi.org/10.1007/s11295-008-0168-7
804 Ritter, E., Rodriguez, M.J.B., Herran, A., Estioko, L., Becker, D., and Rohde, W. (2000). "Analysis
805 of quantitative trait locis (QTL) based on linkage maps in Coconut (Cocos nucifera L.),"
806 in *Plant Genetic Engineering: Towards the Third Millennium,* ed. A.D. Arencibia.), 42-
807 48. <Go to ISI>://WOS:000168743800006

808 Roux, F., Touzet, P., Cuguen, J., and Le Corre, V. (2006). How to be early flowering: an
809 evolutionary perspective. *Trends in Plant Science* 11**,** 375-381.
810 https://doi.org/https://doi.org/10.1016/j.tplants.2006.06.006
811 Sansaloni, C., Petroli, C., Jaccoud, D., Carling, J., Detering, F., Grattapaglia, D., and Kilian, A.
812 (2011). Diversity Arrays Technology (DArT) and next-generation sequencing combined:
813 genome-wide, high throughput, highly informative genotyping for molecular breeding
814 of *Eucalyptus*. *BMC Proceedings* 5**,** P54. http://www.biomedcentral.com/1753-
815 6561/5/S7/P54
816 Santos, G.A., Batugal, P., Othman, A., Baudouin, L., and Labouisse, J.-P. (1996). Manual on
817 standardized research techniques in coconut breeding.
818 Santos, P., Venancio, T.M., Dos Santos, P.H.D., Ramos, H.C.C., Aredes, F.a.S., Azevedo, A.O.N.,
819 Boechat, M.S.B., De Souza, G.A., Ramos, S.R.R., Mirisola, L.A., Aragao, W.M., and
820 Pereira, M.G. (2020). Genotyping-by-sequencing technology reveals directions for
821 coconut (Cocos nucifera L.) breeding strategies for water production. *Euphytica* 216.
822 https://doi.org/10.1007/s10681-020-02582-1
823 Siberchicot, A., Bessy, A., Guéguen, L., and Marais, G.A. (2017). MareyMap Online: A User-
824 Friendly Web Application and Database Service for Estimating Recombination Rates
825 Using Physical and Genetic Maps. *Genome Biology and Evolution* 9**,** 2506-2509.
826 https://doi.org/10.1093/gbe/evx178
827 Van Ooijen, J.W., and Voorrips, R.E. (2001). JoinMap 3.0, Software for the calculation of
828 genetic linkage maps. *P. R. International* Wageningen, The Netherlands.,
829 Voorrips, R.E. (2002). MapChart: Software for the graphical presentation of linkage maps and
830 QTLs. *Journal of Heredity* 93**,** 77-78. https://doi.org/DOI 10.1093/jhered/93.1.77
831 Wang, S., Xiao, Y., Zhou, Z.-W., Yuan, J., Guo, H., Yang, Z., Yang, J., Sun, P., Sun, L., Deng, Y., Xie,
832 W.-Z., Song, J.-M., Qamar, M.T.U., Xia, W., Liu, R., Gong, S., Wang, Y., Wang, F., Liu, X.,
833 Fernie, A.R., Wang, X., Fan, H., Chen, L.-L., and Luo, J. (2021). High-quality reference
834 genome sequences of two coconut cultivars provide insights into evolution of monocot
835 chromosomes and differentiation of fiber content and plant height. *Genome Biology*
836 22**,** 304. https://doi.org/10.1186/s13059-021-02522-9
837 Wei, T., Simko, V., Levy, M., Xie, Y., Jin, Y., Zemla, J., Freidank, M., Cai, J., and Protivinsky, T. (
838 2021). R package 'corrplot': Visualization of a Correlation Matrix (Version 0.92).
839 Wickland, D.P., and Hanzawa, Y. (2015). The FLOWERING LOCUS T/TERMINAL FLOWER 1 Gene
840 Family: Functional Evolution and Molecular Mechanisms. *Molecular Plant* 8**,** 983-997.
841 https://doi.org/10.1016/j.molp.2015.01.007
842 Wilms, H., De Bièvre, D., Longin, K., Swennen, R., Rhee, J., and Panis, B. (2021). Development
843 of the first axillary in vitro shoot multiplication protocol for coconut palms. *Scientific*
844 *Reports* 11**,** 18367. https://doi.org/10.1038/s41598-021-97718-1
845 Xia, W., Liu, R., Zhang, J., Mason, A.S., Li, Z., Gong, S., Zhong, Y., Dou, Y., Sun, X., Fan, H., and
846 Xiao, Y. (2020). Alternative splicing of flowering time gene FT is associated with halving
847 of time to flowering in coconut. *Scientific Reports* 10**,** 11640.
848 https://doi.org/10.1038/s41598-020-68431-2
849 Yang, Y., Bocs, S., Fan, H., Armero, A., Baudouin, L., Xu, P., Xu, J., This, D., Hamelin, C., Iqbal, A.,
850 Qadri, R., Zhou, L., Li, J., Wu, Y., Ma, Z., Issali, A.E., Rivallan, R., Liu, N., Xia, W., Peng,
851 M., and Xiao, Y. (2021). Coconut genome assembly enables evolutionary analysis of
852 palms and highlights signaling pathways involved in salt tolerance. *Communications*
853 *Biology* 4**,** 105. https://doi.org/10.1038/s42003-020-01593-x

854

Table 1. Statistics of the linkage map and its alignment to the two available chromosome-level genome assemblies of coconut (*Cocos nucifera* L.).

LINKAGE MAP				YANG GENOME						WANG GENOME			
LG #	# of link. map SNPs	Total Size (cM)	Mean interSNP dist (cM)	Chr. #	Phys. dist. covered (Mb	Mean interSNP phys. dist. (Mb)	Number of annotated genes#	Average recomb. rate (cM/Mbp)	r^2 (Number of genes and recomb. rate)	Chr. #	Phys. dist. covered (Mb)	Mean interSNP phys. dist. (Mb)	Average recomb. rate (cM/Mbp)
1	329	196.6	0.599 ± 0.470	1	119.197	0.362 ± 0.652	2277	2.27 ± 1.17	0.68	5	177.52	0.570 ± 1.533	2.12 ± 0.94
2	311	199.1	0.642 ± 0.492	2	85.353	0.275 ± 0.411	1997	2.44 ± 0.66	0.72	1	213.40	0.656 ± 2.751	1.97 ± 0.649
3	209	149.2	0.717 ± 0.625	3	82.325	0.396 ± 0.576	1705	1.98 ± 0.65	0.73	4	179.12	0.835 ± 2.527	1.67 ± 1.26
4	222	161.2	0.729 ± 0.536	4	66.748	0.302 ± 0.454	1610	3.05 ± 1.52	0.87	6	170.88	0.762 ± 2.005	2.56 ± 1.46
5	150	147.5	0.989 ± 0.654	5	57.717	0.385 ± 0.624	1104	3.77 ± 2.06	0.89	9	156.70	1.073 ± 5.397	2.98 ± 1.87
6	262	193.4	0.729 ± 0.764	6	81.468	0.311 ± 0.463	2095	2.42 ± 0.74	0.46	3	187.69	0.693 ± 2.894	1.84 ± 0.50
7	215	148.8	0.695 ± 0.686	7	77.453	0.361 ± 0.758	1583	2.13 ± 0.60	0.21	2	188.13	0.776 ± 2.790	1.60 ± 0.76
8	176	95.7	0.547 ± 0.505	8	58.631	0.326 ± 0.668	1214	2.09 ± 1.16	0.77	13	95.96	0.508 ± 1.273	1.56 ± 0.75
9	106	89.9	0.856 ± 0.725	9	59.333	0.554 ± 0.792	1026	2.37 ± 1.33	0.89	11	137.92	1.378 ± 3.871	2.12 ± 1.38
10	144	113.0	0.790 ± 0.493	10	57.105	0.399 ± 0.663	1066	2.90 ± 1.45	0.87	10	144.69	0.969 ± 4.013	2.39 ± 1.53
11	165	72.4	0.785 ± 0.750	11	61.809	0.375 ± 0.617	1379	3.01 ± 1.93	0.61	7	173.86	1.073 ± 3.547	2.64 ± 1.77
12	133	94.9	0.728 ± 0.489	12	42.367	0.302 ± 0.425	868	3.21 ± 1.86	0.86	14	89.87	0.681 ± 2.625	2.88 ± 1.76
13	127	102.6	0.814 ± 0.617	13	60.488	0.479 ± 1.032	847	3.77 ± 2.55	0.87	15	82.46	0.641 ± 1.677	3.63 ± 2.05
14	189	132.8	0.706 ± 0.544	14	56.198	0.296 ± 0.351	1309	3.15 ± 1.35	0.73	8	155.26	0.754 ± 3.799	2.66 ± 1.30
15	101	135.7	1.357 ± 3.139	15	31.114	0.311 ± 0.800	646	5.18 ± 3.33	0.04	12	145.36	1.075 ± 3.394	3.04 ± 1.43
16	113	91.5	0.819 ± 0.664	16	38.139	0.313 ± 0.623	867	3.97 ± 1.48	0.91	16	83.33	0.686 ± 2.239	3.34 ± 1.58
Total	2,952	2,124.3	-		1,035.445	-	21,593	2.79 ± 1.65			2,382.141	-	2.32 ± 1.40
Mean ± s.d.	184.5 ± 69.9	132.8 ± 40.8	0.742 ± 0.471		43.14%	0.349 ± 0.652					99.27%	0.779 ± 2.947	

Number of annotated genes from (Yang et al. 2021; BioProject: PRJNA374600)

Table 2. Summary of QTL mapping results in the coconut F_2 population.

	Days to Launch of First Spathe (DLFS)	Bole emergence (BOLE)	Number of bunches with fruit (NBF)	Petiole Length (PL)
Chromosome	3	3	1	3
LOD score threshold (percentile)	5.14 (99%)	4.47 (95%)	5.14 (99%)	5.14 (99%)
# SNPs in QTL region	52	1	1	22
QTL region position (cM)	118.928 - 149.166	132.62	57.16	123.503 – 136.125
Right SNP	100287206_T>A-55	-	-	100287206_T>A-55
Left SNP	100273632_T>G-15	-	-	100273632_T>G-15
Peak LOD	11.86	4.64	5.68	7.79
Peak LOD SNP	100226499_C>T-34	100228320_G>A-40	100237259_A>G-48	100226499_C>T-34
Target SNP allele	T	A	A	T
(Origin; effect)	(Dwarf; reduction)	(Dwarf; increase)	(Dwarf; increase)	(Dwarf; reduction)
Genome position (bp)	73,147,443	75,613,473	19,206,916	73,147,443
Variance explained (%)	64.0	3.12	0.43	22.3

Figure legends

Figure 1. Alignment of the linkage map (green) to the two chromosome-level genome assemblies, the YANG genome assembly (red) (Yang et al., 2021) and the WANG genome assembly (blue) (Wang et al., 2021).

Figure 2. Marey maps showing the correspondence between the physical position (x-axis, Mb) and the recombination-based position (y-axis, cM) on the 16 Coconut chromosomes of the YANG genome assembly (Yang et al., 2021) and the WANG genome assembly (Wang et al., 2021). Also shown in the intermediate panels the combined pattern of gene density distribution and the LOESS curve of recombination rate for the YANG genome.

Figure 3. Histogram of the coconut phenotypic trait distributions in the F_2 mapping population.

Figure 4. Matrix of genotypic correlations among the measured traits in the F_2 mapping population

Figure 5. Genome-wide QTL mapping profiles for the mapped traits (Y axis) obtained with the three different QTL mapping methods implemented (X axis)

Figure 6. Detailed view of the major effect QTL region for flowering time, petiole length and bole presence in the stem on chromosome 3 of the YANG genome. The *A. thaliana* FLOWERING LOCUS T was colocalized with the leading SNPs for the QTL.

Supplementary material

File S1. DArTSeq SNP genotypic data for the full 3714 linkage mapped SNPs in the F_2 population

File S2. Genotypic data for the 2952 DArTSeq SNP markers linkage mapped and physically mapped to unique positions on the coconut genome assemblies

File S3. BLAST results of the DArTSeq SNP corresponding sequences, target SNP type and position, against the YANG and WANG genomes.

File S4. Local recombination rates estimated following the Marey maps construction and LOESS smoothing between the linkage map and the two assembled genomes

File S5. Raw phenotypic data and estimated BLUPs following the mixed model analysis for the evaluated traits in the F_2 population

File S6. QTL mapping results obtained with the composite interval mapping method

File S7. BLAST alignment results of the *Arabidopsis thaliana* putative flowering signals mediating protein FT (At1g65480) mRNA, complete cds against the YANG chromosome 3

File S8. BLAST alignment results of the *Arabidopsis thaliana* putative flowering signals mediating protein FT (At1g65480) mRNA, complete cds against the WANG chromosome 4

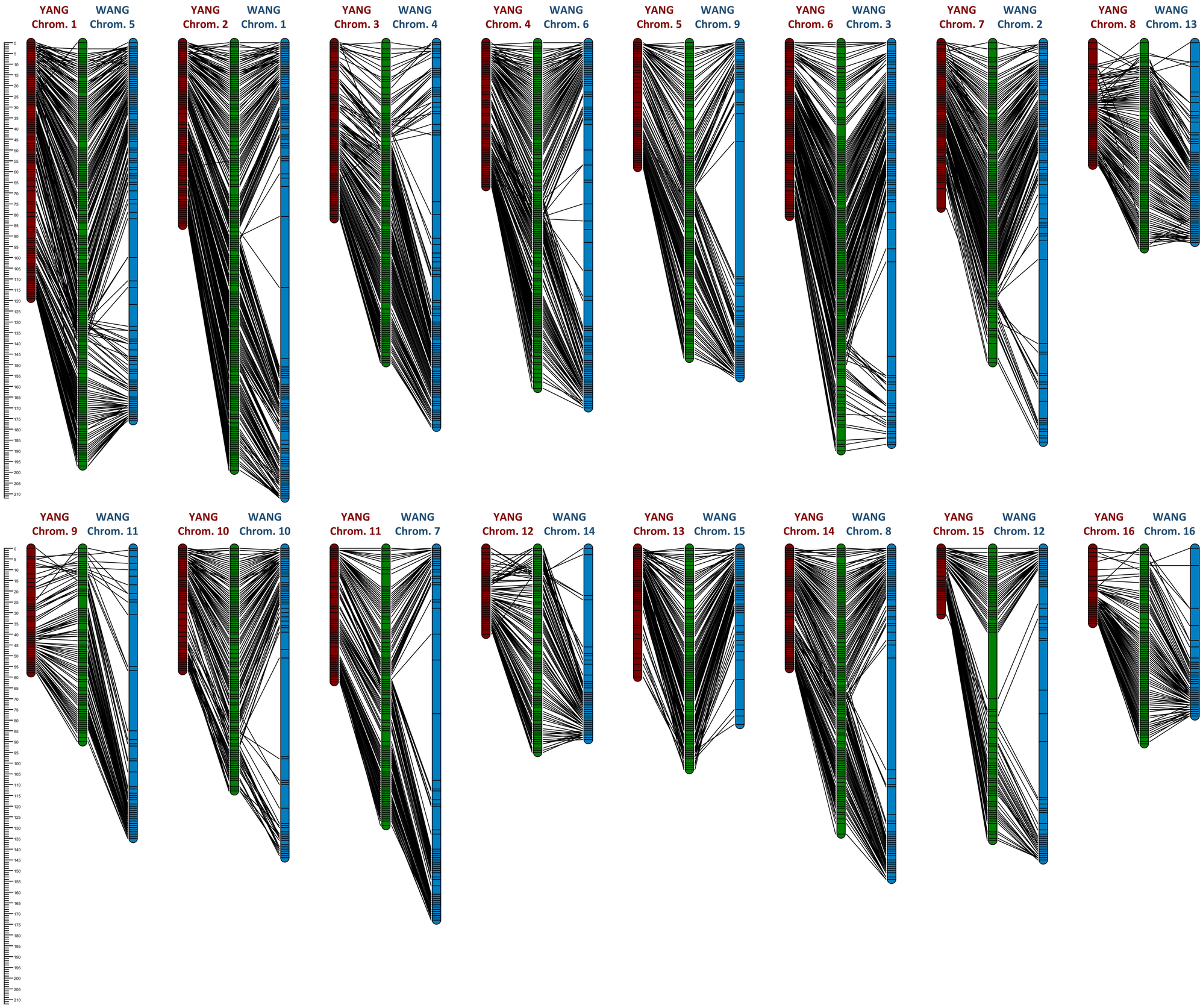
YANG Chrom. 1
WANG Chrom. 5
YANG Chrom. 2
WANG Chrom. 1
YANG Chrom. 3
WANG Chrom. 4
YANG Chrom. 4
WANG Chrom. 6
YANG Chrom. 5
WANG Chrom. 9
YANG Chrom. 6
WANG Chrom. 3
YANG Chrom. 7
WANG Chrom. 2
YANG Chrom. 8
WANG Chrom. 13
YANG Chrom. 9
WANG Chrom. 11
YANG Chrom. 10
WANG Chrom. 10
YANG Chrom. 11
WANG Chrom. 7
YANG Chrom. 12
WANG Chrom. 14
YANG Chrom. 13
WANG Chrom. 15
YANG Chrom. 14
WANG Chrom. 8
YANG Chrom. 15
WANG Chrom. 12
YANG Chrom. 16
WANG Chrom. 16

Chrom. 1 YANG

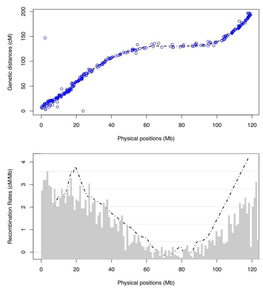

Chrom. 2 YANG

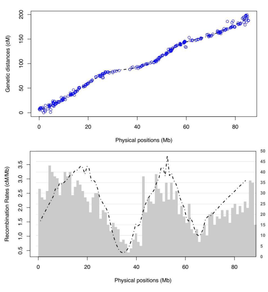

Chrom. 3 YANG

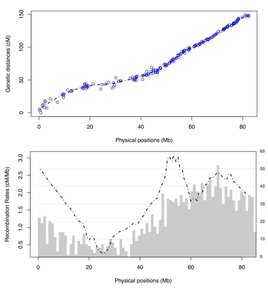

Chrom. 4 YANG

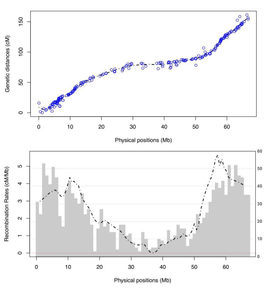

Chrom. 5 WANG

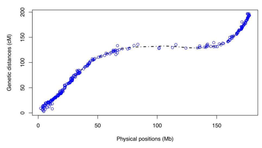

Chrom. 1 WANG

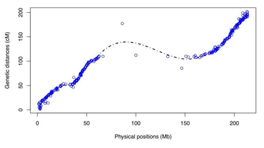

Chrom. 4 WANG

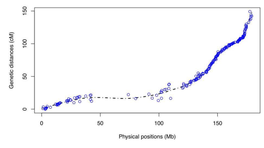

Chrom. 6 WANG

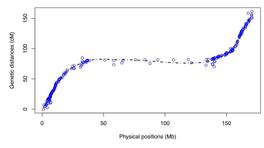

Chrom. 5 YANG

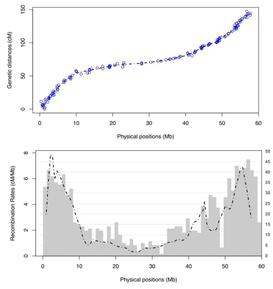

Chrom. 6 YANG

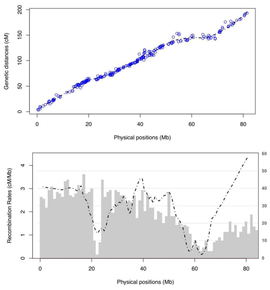

Chrom. 7 YANG

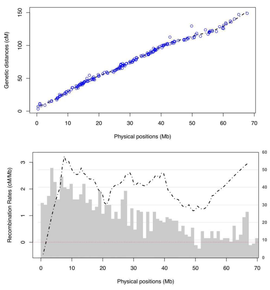

Chrom. 8 YANG

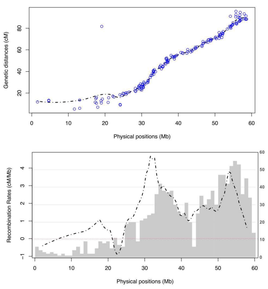

Chrom. 9 WANG

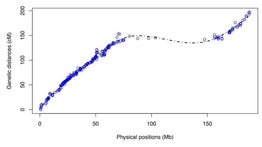

Chrom. 3 WANG

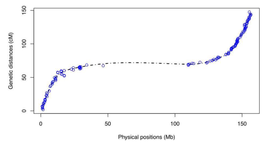

Chrom. 2 WANG

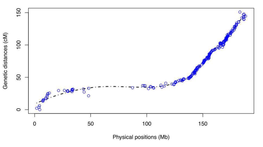

Chrom. 13 WANG

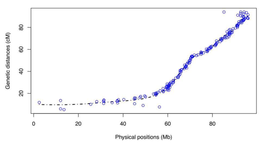

Chrom. 9 YANG

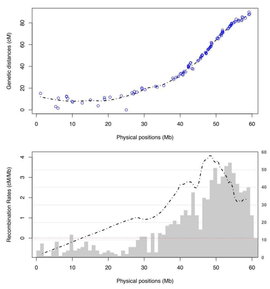

Chrom. 10 YANG

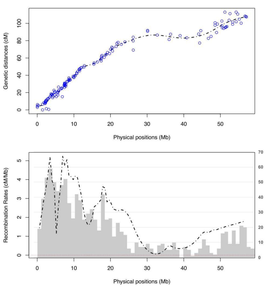

Chrom. 11 YANG

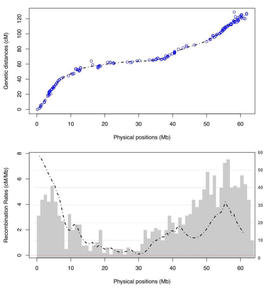

Chrom. 12 YANG

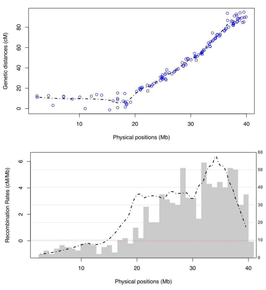

Chrom. 11 WANG

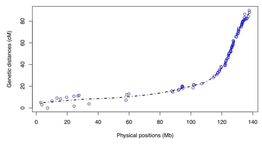

Chrom. 10 WANG

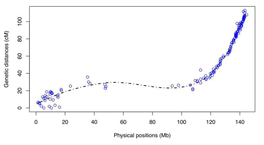

Chrom. 7 WANG

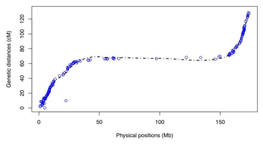

Chrom. 14 WANG

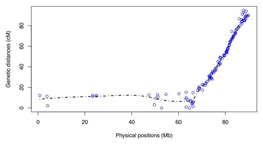

Chrom. 13 YANG

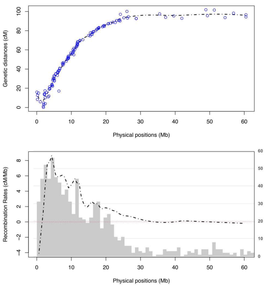

Chrom. 14 YANG

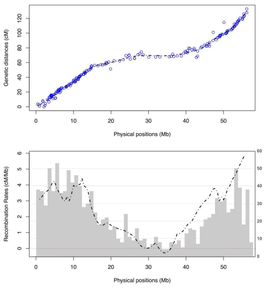

Chrom. 15 YANG

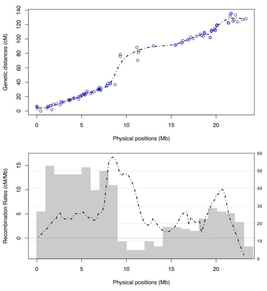

Chrom. 16 YANG

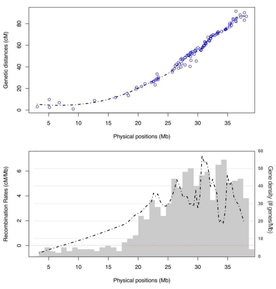

Chrom. 15 WANG

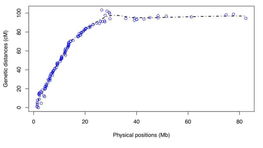

Chrom. 8 WANG

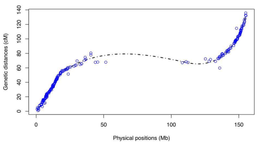

Chrom. 12 WANG

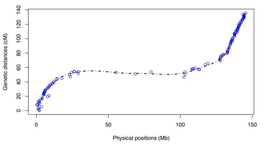

Chrom. 16 WANG

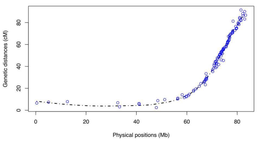

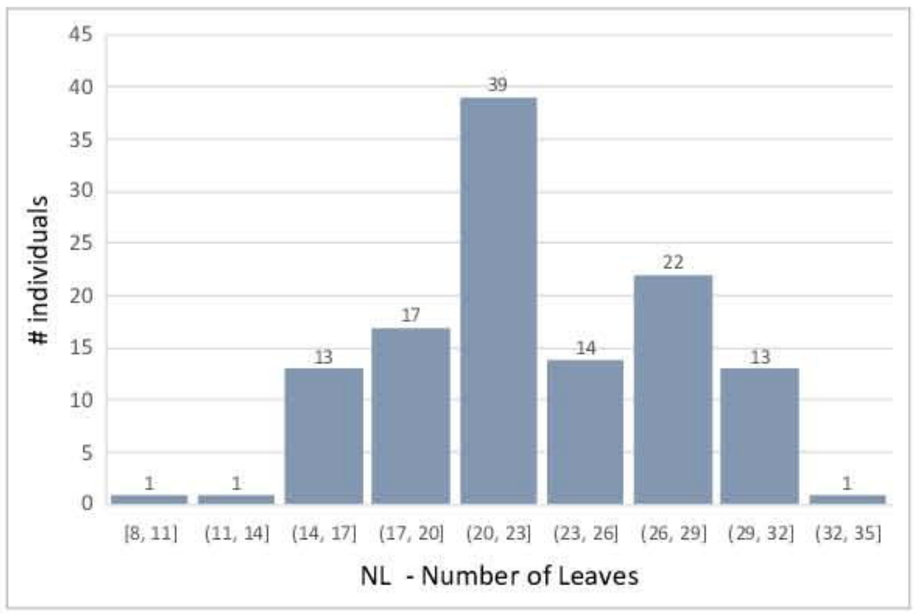
individuals
NL - Number of Leaves

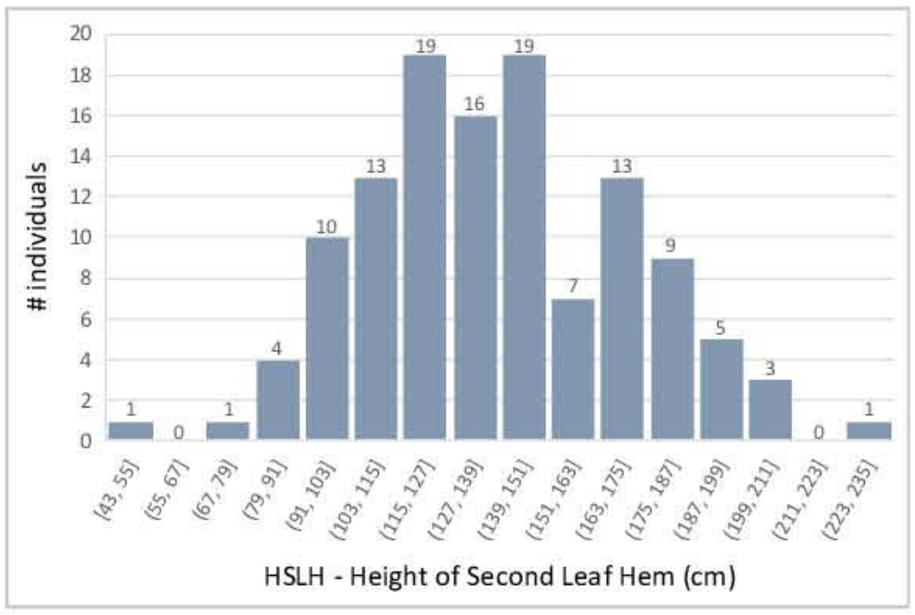
individuals
HSLH - Height of Second Leaf Hem (cm)

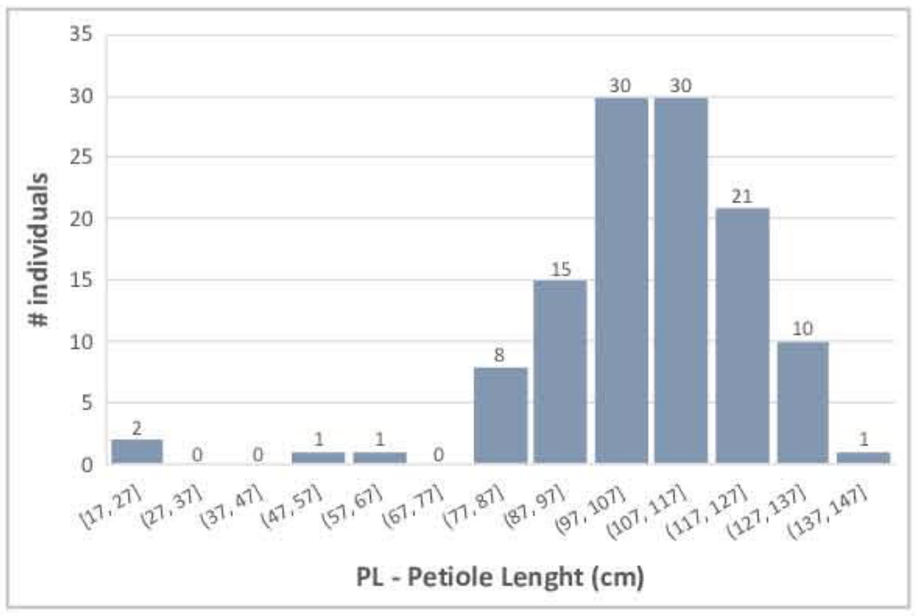
individuals
PL - Petiole Lenght (cm)

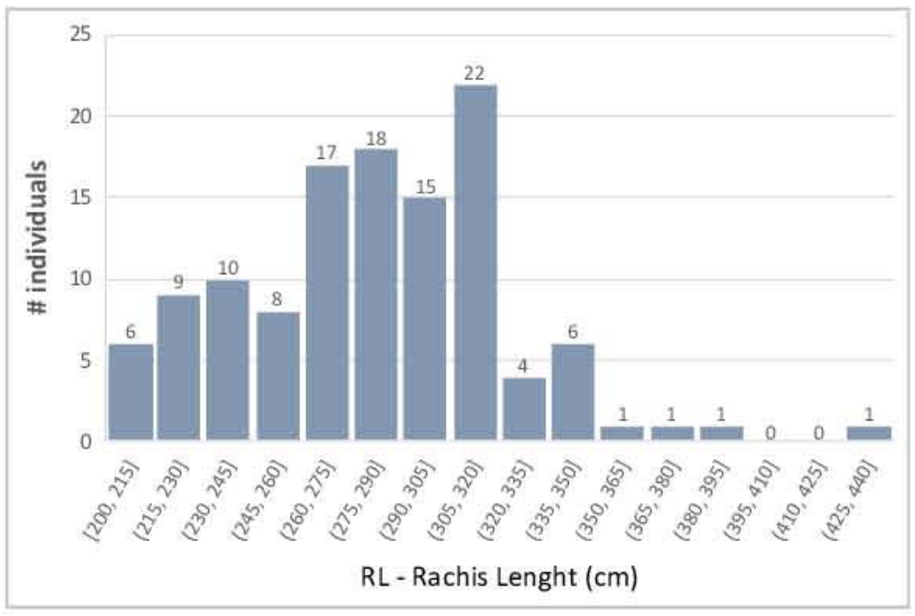
individuals
RL - Rachis Lenght (cm)

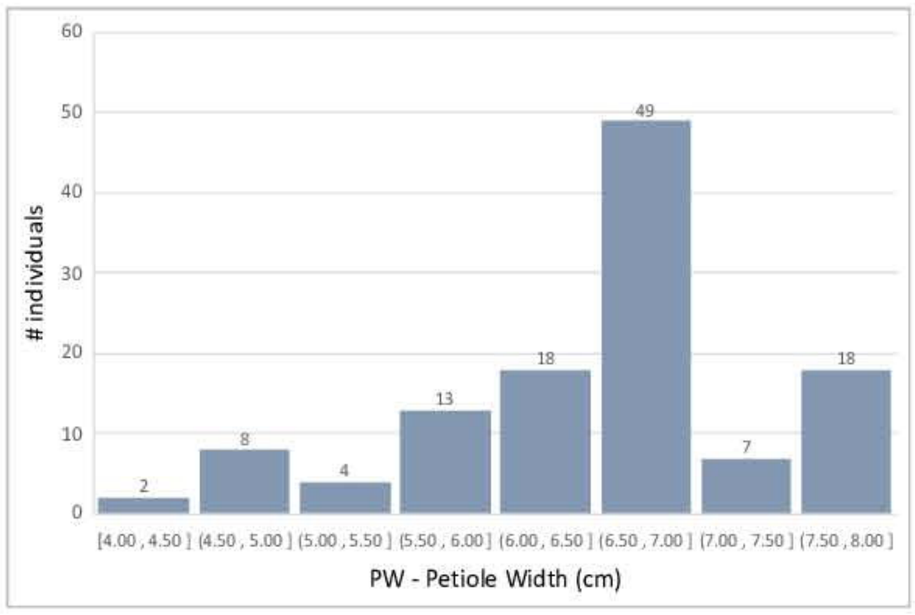
individuals
PW - Petiole Width (cm)

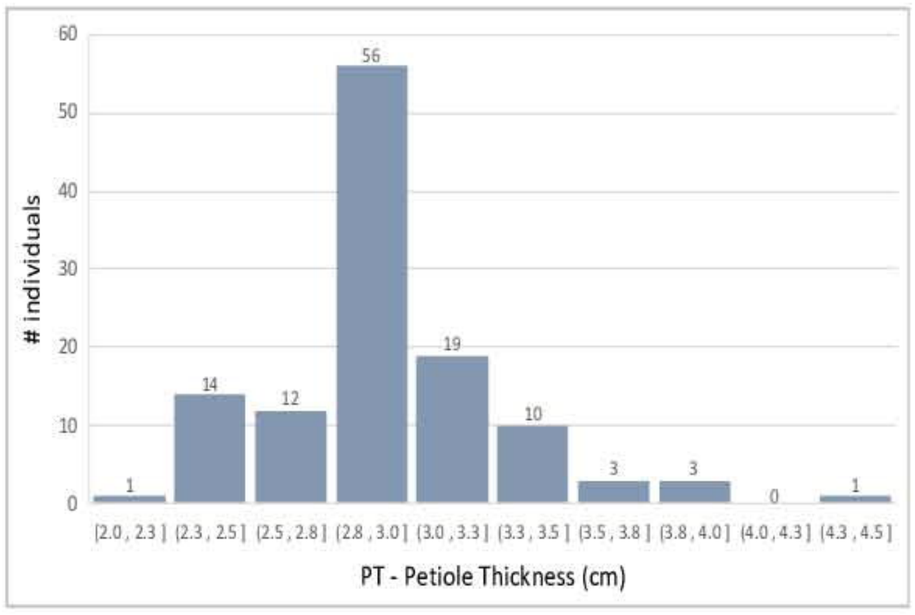
individuals
PT - Petiole Thickness (cm)

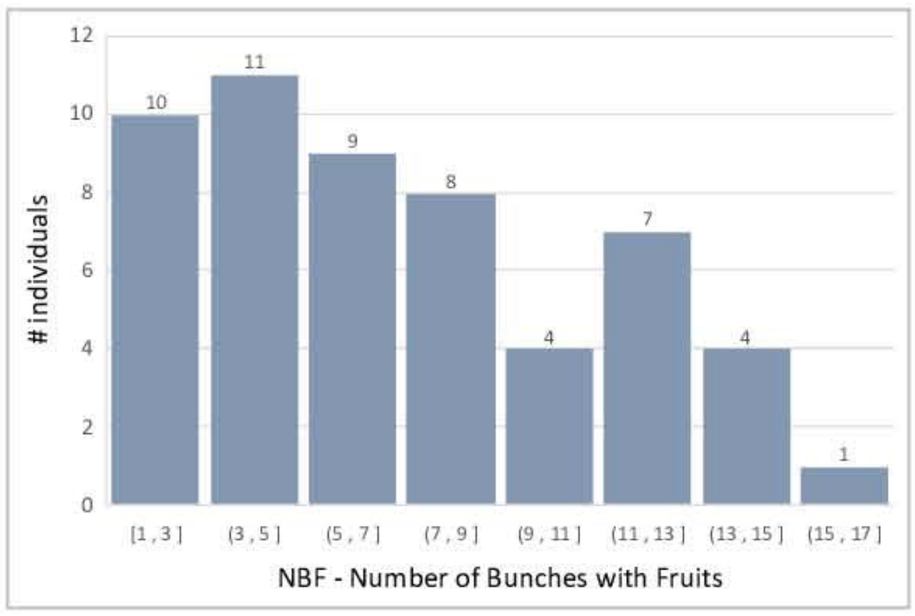
individuals
NBF - Number of Bunches with Fruits

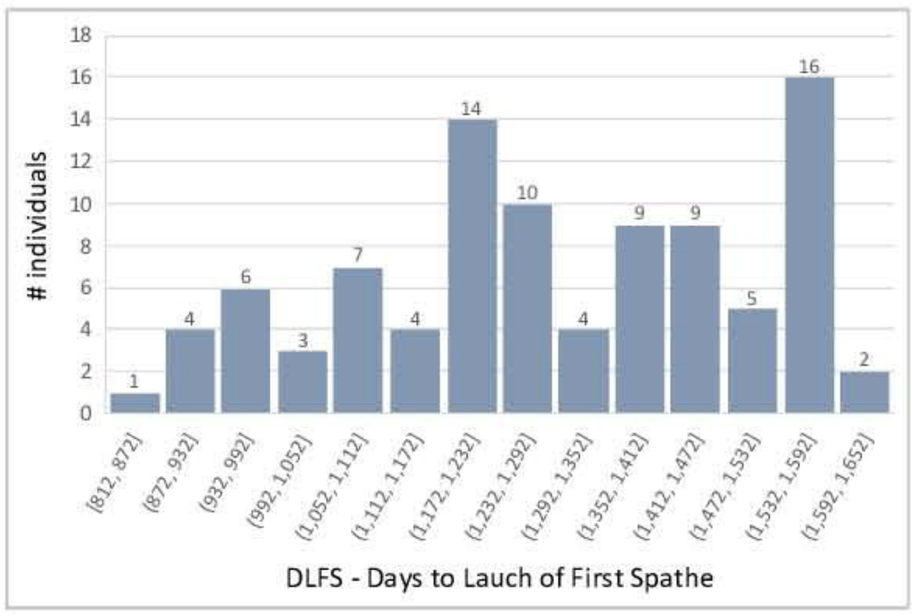
individuals
DLFS - Days to Lauch of First Spathe

	HSLH	PL	RL	PW	PT	BOLE	NBF	DLFS
NL	0.772	-0.091	0.519	0.368	0.224	0.368	0.421	-0.484
HLH		0.119	0.706	0.435	0.362	0.430	0.369	-0.349
PL			0.043	0.053	0.146	-0.207	-0.348	0.479
RL				0.514	0.505	0.292	0.255	-0.132
PW					0.403	0.141	0.066	-0.067
PT						0.081	-0.044	0.110
BOLE							0.347	-0.417
NBF								-0.519

HK – Haley Knott regression

IM - Interval Mapping

Non-parametric IM

DLFS - Days to Launch of First Spathe

BOLE emergence

PL – Petiole Length

NBF - Number of Bunches with Fruit

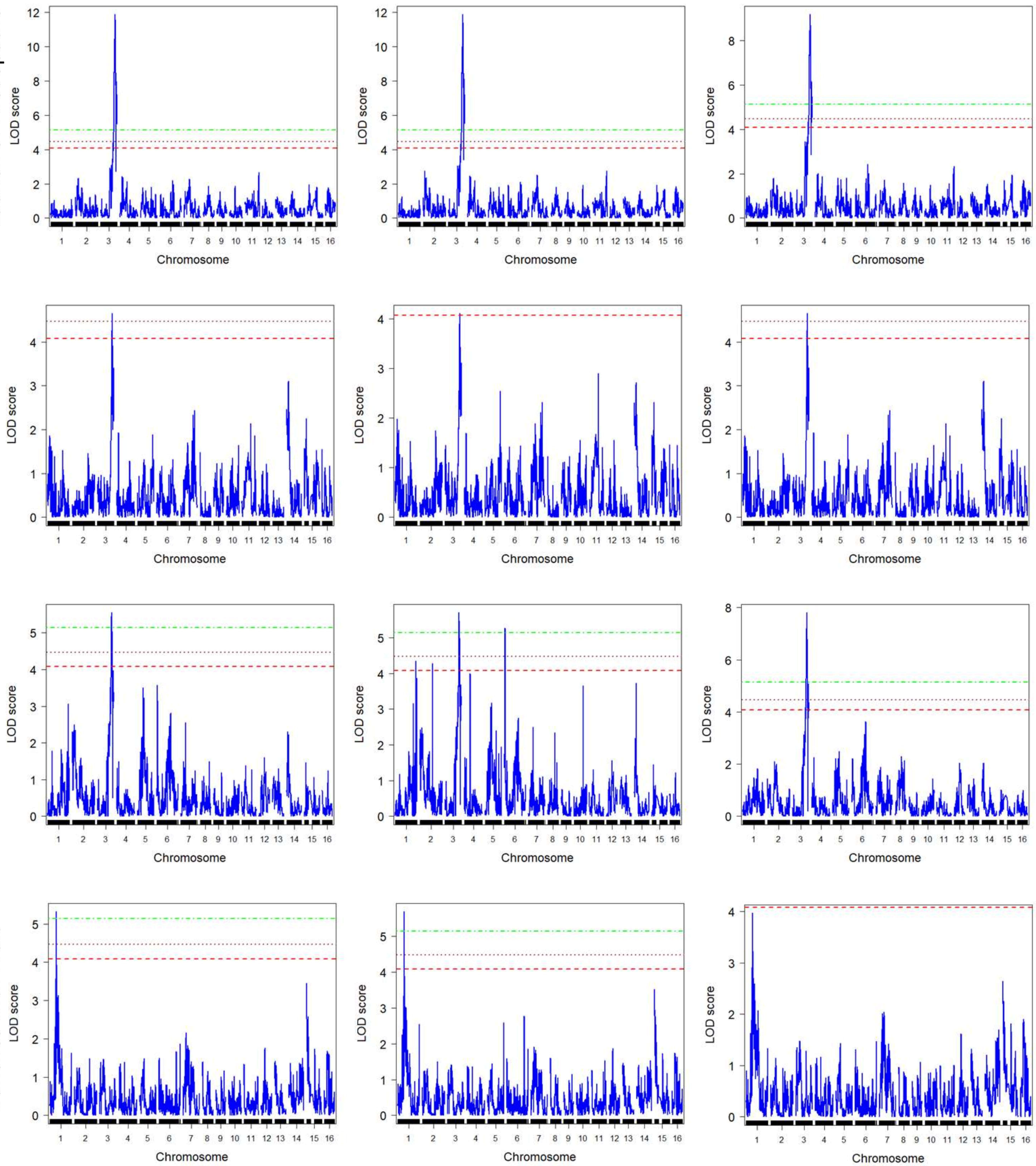

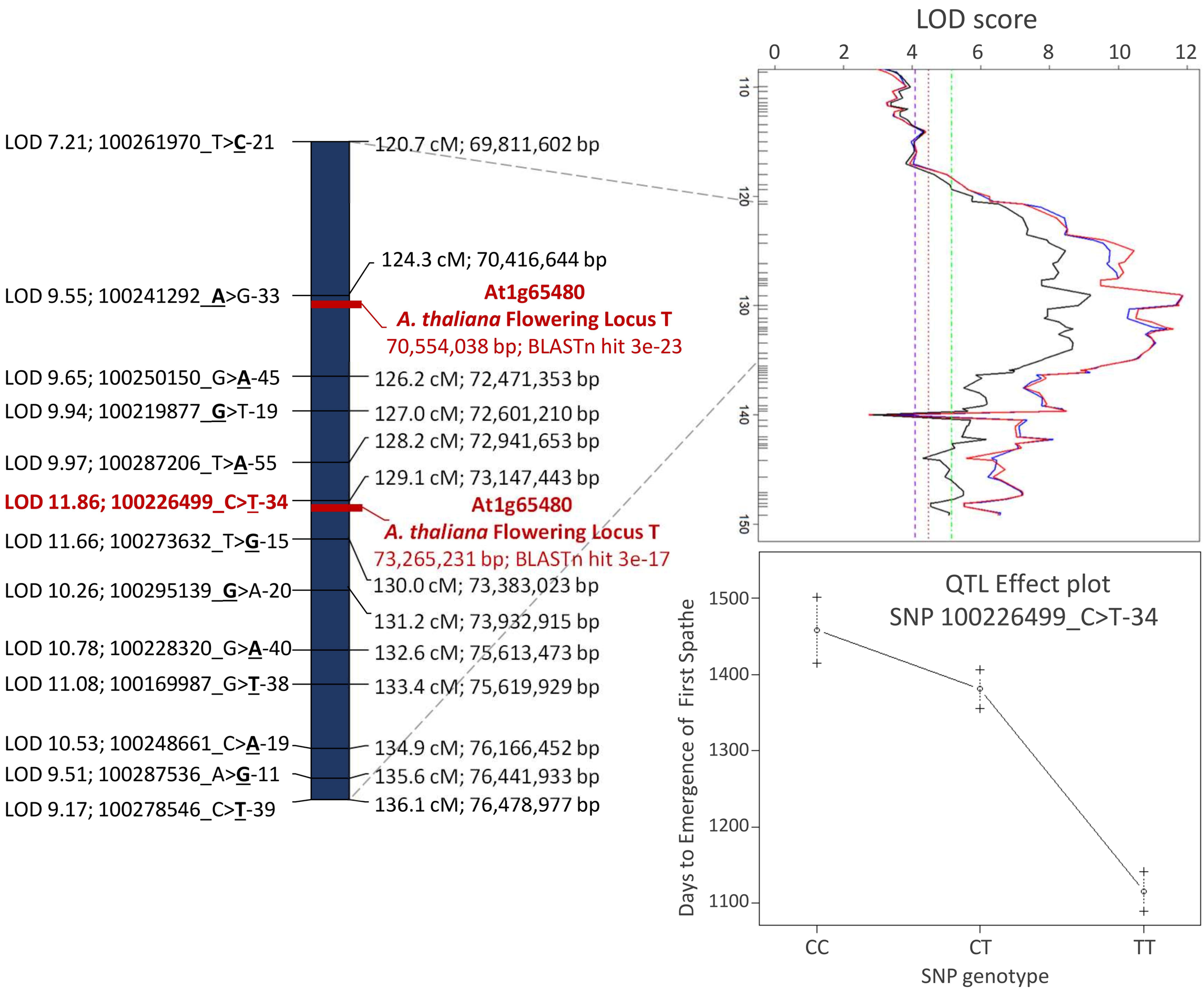
LOD score
0
2
4
6
8
10
12
110
120
130
140
150
LOD 7.21; 100261970_T>C-21
120.7 cM; 69,811,602 bp
124.3 cM; 70,416,644 bp
LOD 9.55; 100241292_A>G-33
At1g65480
A. thaliana Flowering Locus T
70,554,038 bp; BLASTn hit 3e-23
LOD 9.65; 100250150_G>A-45
126.2 cM; 72,471,353 bp
LOD 9.94; 100219877_G>T-19
127.0 cM; 72,601,210 bp
128.2 cM; 72,941,653 bp
LOD 9.97; 100287206_T>A-55
129.1 cM; 73,147,443 bp
LOD 11.86; 100226499_C>T-34
At1g65480
A. thaliana Flowering Locus T
73,265,231 bp; BLASTn hit 3e-17
LOD 11.66; 100273632_T>G-15
130.0 cM; 73,383,023 bp
LOD 10.26; 100295139_G>A-20
131.2 cM; 73,932,915 bp
LOD 10.78; 100228320_G>A-40
132.6 cM; 75,613,473 bp
LOD 11.08; 100169987_G>T-38
133.4 cM; 75,619,929 bp
LOD 10.53; 100248661_C>A-19
134.9 cM; 76,166,452 bp
LOD 9.51; 100287536_A>G-11
135.6 cM; 76,441,933 bp
LOD 9.17; 100278546_C>T-39
136.1 cM; 76,478,977 bp
QTL Effect plot
SNP 100226499_C>T-34
Days to Emergence of First Spathe
1500
1400
1300
1200
1100
CC
CT
TT
SNP genotype